RSC Advances

REVIEW

View Article Online
View Journal | View Issue

Cite this: *RSC Adv.*, 2026, **16**, 24482

Ion-exchange functionalized polystyrene-based composites: synthesis, conductive hybridization, and environmental applications

Amany A. El Mansoub, *[ab] Rasha M. El Nashar, [a] Hussein M. Fahmy,[a] Heba A. Hani,[b] Abdelghani M. G. Abulnour[b] and Marwa M. El Sayed[b]

Polystyrene is the oldest and most widely used synthetic polymer, and it is divided into two main types: expanded polystyrene (EPS) and general-purpose polystyrene (GPPS). This versatile material is used in various commercial applications. One of the challenges with polystyrene is its hydrophilicity, which can be addressed through functionalization, enhancing its overall properties. Polystyrene-based resins have significant advantages over natural organic ion exchangers. These resins, when incorporated into nanocomposites, demonstrate excellent reshaping and performance in ion exchange (IEX) materials, particularly for water treatment applications. The combination of IEX with nanomaterials has the potential to further improve effectiveness. Low-dimensional carbon materials, including carbon nanotubes, graphene derivatives, metal oxides, and silica, exhibit potential for improving the properties of ion exchange materials at the laboratory scale. This study reviews recent advancements in polystyrene copolymerization, the use of nanofillers, and the integration of polymeric and superconducting additives to improve functional performance. In addition, it offers a systematic evaluation of existing constraints techniques in polystyrene-based ion-exchange nanocomposites for environmental applications. Several factors characterise conductive and superconductive materials. Organic polymer matrices with superconducting nanoparticles form superconductive polymeric nanocomposites. Electrical impedance and diamagnetic response are the main superconducting tests for these materials. Polystyrene composites' superconductivity comes from ceramic superconductor particles, not the polymer. Interfacial interactions and conduction processes among filler particles affect their performance. This review emphasizes the production of polystyrene-based nanocomposites and their potential as advanced adsorbents while identifying research gaps and key findings in the field.

Received 14th January 2026
Accepted 26th April 2026

DOI: 10.1039/d6ra00347h

rsc.li/rsc-advances

1. Introduction

Synthetic petrochemical-derived polymers like polyethylene (PE), polypropylene (PP), and polystyrene (PS) exhibit diverse chemical and structural properties, making them suitable for various applications.[1] PS, a key synthetic polymer, is produced through the polymerization of styrene and can be either solid or brittle, depending on processing methods. It is categorized into EPS and GPPS, applied in bags, bottles, building materials, insulation, and medical supplies.[2] Commonly, PS appears as a transparent latex or pale yellow plastic characterized by intermingled, randomly coiled polymer chains.[3]

Functionalizing polystyrene enhances hydrophilicity for aqueous environments *via* bulk or surface treatments, using methods like plasma, laser, or UV radiation combined with oxygenated or aminated compounds.[4] PS microspheres are produced through various techniques, including emulsion and seed polymerization. Compared to bulk PS, micro-sized particles offer improved stability under heat and can immobilize polymer chains. Incorporating nanoparticles, created through microemulsion and liquid slurry polymerization, further enhances material characteristics by providing heat stability, high surface area, effective interactions, and improved mechanical properties.[5]

Sulphonated cross-linked polystyrene (SPS) is a highly acidic, hygroscopic gel. Its swelling and shrinking ability in water depends on the degree of cross-linking. Styrene and divinylbenzene (DVB) are copolymerized into beads, which are sulphonated with concentrated sulfuric acid at 100 °C in the presence of silver sulfate.[6] The fiber form of highly sulfonated polystyrene is suitable for ion-exchange applications due to its conductive pathways.[7] Cation exchange membranes are synthesized using a green method that avoids organic solvents, integrating lithium styrene sulfonate into porous supports.[8] Aminated hyper-crosslinked polystyrene porous adsorbent

[a]*Chemistry Department, Faculty of Science, Cairo University, Egypt. E-mail: aa.el-mansoub@nrc.sci.eg; amany.elmansoup@gmail.com*
[b]*Chemical Engineering and Pilot Plant Department, National Research Centre, Cairo, Egypt*

(HCP-DFDA) is functionalized with tertiary amine groups and shown to effectively capture medium- to large-sized blood toxins, presenting a promising alternative for treating uremia.[9]

This review discusses advancements in polystyrene-based polymers, including copolymerization, the use of nanofillers (such as metals, clays, and silica), and conductive additives (including polyaniline and carbon nanoparticles) from 2018 to 2025. Recent reviews offer insights into recycling polystyrene (PS) and ecotoxicological research on polystyrene nanoparticles is also examined.[1,10–12] This review also devotes sections to discussing the conductive hybridization as follows. The differences between conductive and superconductive materials are often characterized by attributes such as electrical resistance, critical temperature, magnetic field response, critical current density, and energy gap.[13–17] Superconductive polymeric nanocomposites are hybrid materials that combine organic polymer matrices with superconducting nanoparticles or fillers.[14,15] The electrical impedance and diamagnetic response techniques are the predominant approaches for assessing superconductivity in polystyrene nanocomposites. The incorporation of polymer chains into the grain structures of ceramics enables their electrical conductivity. Numerous significant researches employ various measurement approaches, as indicated by the available information.[18–25] Incorporating fundamental processes of conductivity and superconductivity, such as the following: two factors that are interconnected affect the electrical performance of conductive composites composed of polystyrene: the interfacial interactions at the polymer–filler interface and the conduction processes among the filler particles that form particle networks[26–33] The development of superconductivity in PS composites is a distinct phenomenon, arising not from the polymer itself but from the integration of ceramic superconductor particles (YBCO) within the PS matrix.[18,19,21]

A thorough examination of PS nanocomposites was conducted between 2015 and 2017. Haider (2017) examines the findings and advancements related to polystyrene and nanoclay-based nanocomposites.[34] Meer (2016) highlights polymer microspheres and silica nanoparticles as key fillers in composites.[35] Afzal (2016) notes growing interest in polystyrene-based materials due to their industrial applications, as various nanofillers enhance their performance.[36] Nasir (2015) explored materials derived from polystyrene and different types of nanoparticles.[37] Previous reviews, such as Nasir (2015), Afzal (2016), and Haider (2017), have predominantly focused on the mechanical, thermal, electrical, and packaging applications of polystyrene nanocomposites. This review of polystyrene-based nanocomposites differs from earlier studies by focusing on ion-exchange-functionalized systems. It highlights recent advancements in polystyrene copolymerization and nanocomposite fabrication since 2017, as well as the integration of low-dimensional nanomaterials, including carbon nanotubes and graphene. The review emphasizes the application of polystyrene nanocomposites for adsorption-focused environmental remediation, particularly in water purification. Additionally, it discusses multifunctional hybrid additives, including superconductors.

Various functionalization and strengthening processes have been reported in the literature to enhance the performance of polystyrene composites in various applications, particularly adsorption. Fig. 1 provides a classification of these strategies. The introduction of charged active sites during surface functionalization by sulfonation and amination improves electrostatic interaction and ion-exchange capacity against ionic contaminants. Reinforcement of stability, swelling behaviour, and adsorption site accessibility is achieved through the incorporation of hydrophilic and crosslinking polymer components including divinylbenzene, poly(acrylamide), poly(acrylonitrile), polyvinylpyrrolidone, polyurethane, and poly(maleic anhydride). Additional hydroxyl and amino groups that facilitate coordination with metal ions are provided by natural biopolymers, such as lignocellulosic materials and chitosan. Metallic particles, zirconium phosphate, magnetite, iron oxide, and titanium dioxide are inorganic additions that can increase the number of adsorption sites by complexing with surfaces and perhaps adding magnetic or catalytic properties. Because of their large surface area and ion-exchange capability, layered silicate minerals such zeolites, nanoclay, organoclay, and kaolin improve adsorption. Also, silica and nano-silica boost surface hydroxyl density and make functional groups more dispersed. Electro-assisted adsorption–

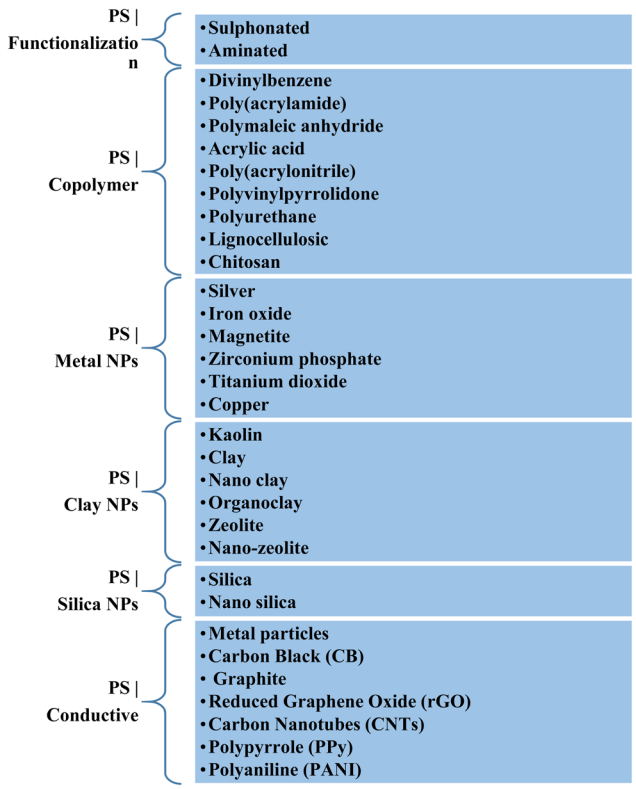

Fig. 1 Classification of functionalization strategies reported for composite adsorbents based on polystyrene, with an emphasis on the contributions of carbon-based conductive materials, clay/zeolite structures, silica phases, and polymer modifiers to improve its application specially, adsorption by means of ion exchange, surface complexation, pore structure development, conductivity, and electrostatic interaction.

desorption applications greatly benefit from the π–π interactions and large surface area provided by carbon-based nanostructures like graphite, reduced graphene oxide, carbon black, and carbon nanotubes, as well as the enhanced electrical conductivity provided by conductive polymers like polypyrrole and polyaniline. Polystyrene composites can have their physicochemical properties fine-tuned to enhance regeneration performance and adsorption efficiency through the use of various modification procedures. Fig. 2 summarizes research development trends in polystyrene composite modification approaches reported between 2020 and 2026 across the various material categories mentioned above. These strategies for modification closely align with these trends.

2. Polystyrene copolymer blends

Polystyrene-based resins are essential for many commercially available resin products, providing notable benefits compared to older natural organic exchangers. By modifying their composition, these resins can be optimized for consistent particle size, cross-linking, and functional group content, resulting in a variety of stable, spherical products.[38]

Blended polystyrene has proven effective in cleaning up oil spills by leveraging the hydrophobic properties and advantages of its original polymers. It is significantly more effective than commercially available sorbents for addressing various types of oil spills. Blends of PS, such as those created from polyethylene and polyvinyl chloride mixed with polystyrene, have been used successfully in the cleanup of numerous oil spills. All fibrous sorbents exhibit a strong affinity for removing crude oil, motor oil, and diesel spills.[39] Transforming a hydrophilic lignocellulosic substance into an oleophilic adsorbent was accomplished by applying cationic surfactants such as cetyltrimethylammonium bromide (CTAB). One study focused on extracting emulsified oil from wastewater using a composite made of polystyrene waste and surfactant-modified bagasse.[40] Electrospun polystyrene fiber mats have high sorption capacity and oil–water selectivity. Polyblend mats with PS and thermoplastic PU fibers promote micro/nano-scale interactions between the polymers.[41]

The ion exchange film made from gum ghatti-grafted poly(acrylamide) copolymer composites (m-PE-g-PS-SO_3H) is highly effective in removing Th(IV) ions from wastewater. This process involves chemically grafting styrene monomer onto a low-density polyethylene film that also contains ethylene propylene diene monomer rubber (PE/EPDM). This is followed by a sulfonation process. In another method, polystyrene foam that is functionalized with chitosan and dithiocarbamate is used to remove mercury from water-based solutions. Additionally, chitosan granules are coated with glutaraldehyde for complete crosslinking and carbon disulfide for functionalization. These modifications lead to an increase in surface area, porosity, and average pore diameter in the final composite. Effective removal of water contaminants is achieved using bionanocomposites that contain nanoparticles doped with chitosan. The amino functional groups in chitosan become protonated, forming stronger bonds with anionic contaminants in acidic environments. Physical treatment of chitosan further enhances its surface area and porosity. Moreover, using chitosan-modified recycled expanded polystyrene nanofibers to remove lead(II) from water is environmentally beneficial, as it transforms waste polymer into an effective metal adsorbent.[42] Moreover, hollow microspheres of polystyrene–polymaleic anhydride (PSMM-NH_2), characterized by a high density of amino groups, have been synthesized and utilized for the efficient adsorption of anionic dyes, with a maximum adsorption capacity of 951.1 mg g^{-1} for acid red. The protonation and deprotonation of amino groups at varying pH levels might alter the surface potential of the produced adsorbent, facilitating its regeneration.[43] A highly efficient poly(acrylonitrile-co-styrene/pyrrole) polyvinylpyrrolidone (poly(AN-co-ST/Py) PVP) has been used for the adsorption of methylene blue dye through the phase inversion method. The process for preparing the copolymers illustrated in Fig. 3, involves precipitating the solution by adding acrylonitrile (AN), pyrrole (Py), and styrene (ST) monomers to a potassium persulfate (KPS) alcoholic solution. This is followed by filtration, washing, and drying.[44] Examples of PS-copolymer blends applied as adsorbents for water treatment are given in Table 1.

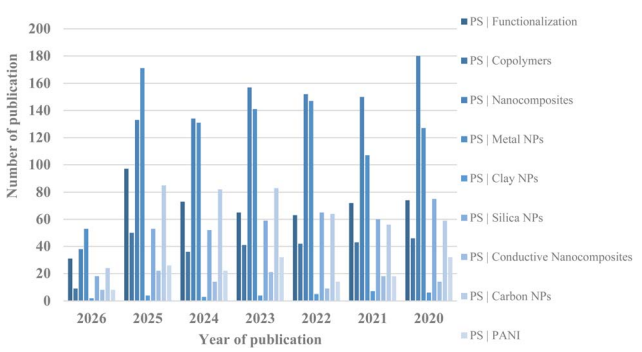

Fig. 2 Timeline chart of reviewing polystyrene different categories from 2020 to 2026.

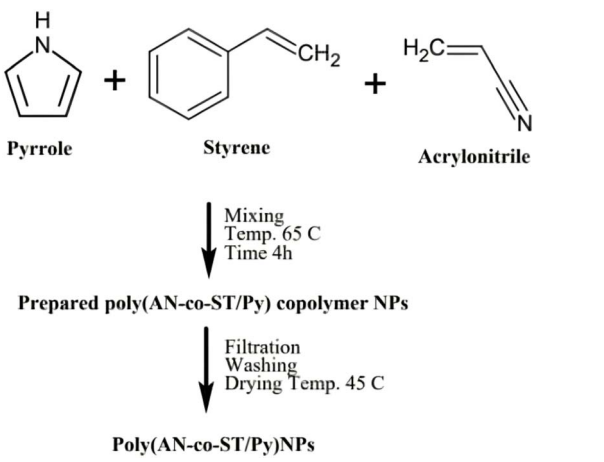

Fig. 3 Preparation of poly (acrylonitrile-co-styrene/pyrrole) copolymer.

Table 1 PS copolymer blends applied for water treatment

Co-polymer	Synthesis conditions	Pollutant	Adsorption conditions	Performance efficiency	References
Polyethylene (PE), and ethylene propylene diene monomer rubber (EPDM)	Grafting copolymerization of styrene onto modified PE at (50–90 °C) for (1–10 h), followed by sulfonation	Thorium ions Th(IV)	pH 3 Temp. 298 K Time 60 min	Grafting yield 130% IEC 1.2 meq g^{-1} Th-Qe 177.5 mg g^{-1} Reusability: 5 cycles Langmuir Pseudo-second-order	48
Aminophosphinic acid (AAP)	Chemical modification using phenylphosphinic acid and propylamine (AAP1), benzylamine (AAP2) and, butylamine (AAP3) at 55 °C, for 30 h	Acetylsalicylic acid (AS)	Dose 8 g L^{-1} Ci 0.5 g L^{-1} Temp. 298 K Time 4 h	Efficiency: AAP1 > AAP3 > AAP2 AS-Qe 42.52 mg g^{-1} R 85% Langmuir Pseudo-second-order	46
Poly (acrylonitrile -co-styrene/pyrrole) (AN-co-ST/Py), and poly vinyl pyrrolidone (PVP)	Precipitation polymerization technique for 4 h at 65 °C followed by mixing with PVP at 60 °C	Cationic methylene blue (MB) dye	Dose 1.6 mg per l pH 11 Time 180 min	MB-Qe 4.087 mg g^{-1} R 90% Reusability: 6 cycles Langmuir Pseudo-second order	44
Styrene–acrylic acid copolymers	Conventional free radical polymerization heated to 80 °C, for 6 h and followed by a sulfonation of styrene (acrylic acid 25%–sulfonated styrene 75%)	Ammonium (NH_4^+)	Ci (5–100) mg L^{-1}	NH_4^+-Qe 55.8 mg g^{-1} R 95.2% Reusability: 5 cycles Freundlich	45
Chitosan/dithicarbamate	Chemical treatment using crosslinked chitosan, then glutaraldehyde and carbon disulfide for 1 h	Mercury (Hg^{2+})	Time 30 min pH 7 Dose 1 g L^{-1} Ci 50 mg per L pH 4	Hg^{2+}-Q_{Max} 1058 mg g^{-1} R 79.85% Reusability: 3 cycles Dubinin–Radushkevich Pseudo-second-order	49
Chitosan	Immersing PS nanofibers in chitosan solution by centrifugal spinning for 10 min	Lead (Pb II)	Time 12 h Dose 1 g L^{-1} Ci 50 mg per L pH 6 Temp. 303 K Time 240 min	Pb(II)-Qe 28.86 mg g^{-1} Q_{Max} 137.35 mg g^{-1} R 61.19% Reusability: 4 cycles Aranovich–Donohue Pseudo-second-order	42
Polymaleic (anhydride)	Addition of *N*,*N*-methylenebis (acrylamide) (MBAA) to form styrene–maleic anhydride copolymer (PSM)/polystyrene–polymaleic (anhydride) (PSMM-NH_2) into core–shell structures	Anionic acid red (AR) dye	Dose 0.1 g L^{-1} Ci 150 mg per L pH 3 Temp. 25 °C	AR – Q_{Max} 951.1 mg g^{-1} R 99% at – filtration 4000 L m^{-2} - Average flux 3000 L m^{-2} h^{-1} Adsorption rate 4.76×10^{-3} g mg^{-1} min^{-1} Reusability: 5 cycles	43
		Oil–water separation	Time 12 h	Langmuir Pseudo-second-order	
Polyurethane (PU)	Polymer blending PS : PU (9 : 1) & electrospun in DMF/THF (4 : 1) using high voltage at RT for more than 24 h	Oil–water selectivity	oil/seawater: 20 g/150 mL Fiber mass 0.15 g Time 2 min	Motor oil – Q_{Max} 144.52 g g^{-1}	41
Surfactant modified bagasse	NaOH-treated bagasse mixed with cetylpyridinium bromide (CTAB) solution at 60 °C for 24 h. Then added to polystyrene waste solution for 1 h	Emulsified food oil from wastewater	Dose 2 g L Ci 2 g L^{-1} pH 5 – 8 Temp. 25 °C Time 2 h	Oil-Qe 22.3 g g^{-1} R 98.7% Reusability: 5 cycles Freundlich	40

Random free radical polymerization and styrene sulfonation yield styrene–acrylic acid copolymers in various ratios. The copolymer composed of acrylic acid and sulfonated styrene exhibited the highest ammonium adsorption capacity at 55.8 mg g^{-1}. This enhanced capacity is attributed to the electrostatic attraction between positively charged NH_4^+ ions and the negatively charged $-COO^-$ and $-SO_3^-$ groups in the copolymer.[45] In addition, poly(styrene-co-divinylbenzene), functionalized with aminophosphinic acid pendant groups, serves as a high-performance adsorbent for acetylsalicylic acid.[46] Reversible addition–fragmentation chain transfer (RAFT) polymerization has successfully produced a high molecular weight polystyrene–polyaniline copolymer with low polydispersity, suitable for carbon-based electrodes in energy storage and other applications that require materials with high carbon yields and controlled porosity structures.[47]

3. Polystyrene nano-composites

This text provides a critical overview of the production of nanocomposites based on polystyrene, focusing on their potential as advanced adsorbents. It evaluates the existing research gaps and summarizes the findings and advancements related to nanocomposite ion exchange (IEX) materials for water treatment. Additionally, the incorporation of low-dimensional carbon materials such as carbon nanotubes, graphene and its derivatives, as well as metal oxides and silica demonstrates promising enhancements in the properties of ion exchange materials at the laboratory scale.[50] Table 2 summarizes the research on polystyrene-nanoparticle adsorbent composites, illustrating the nano filler used, composite synthesis conditions, pollutants removed, adsorption conditions, isotherm and kinetics fitting models, and performance efficiency.

Nanocomposites made from polystyrene have been developed for use in thermoresponsive, electroactive, and photoactive materials. These nanocomposites incorporate carbon nanotubes, graphene, nanoclay, nanoceramics, and metal nanoparticles, showcasing impressive shape-reversal capabilities and excellent performance. Recent applications of shape memory polystyrene-based nanocomposites include the textile industry, drug delivery systems, tissue engineering, and anti-corrosion coatings for metals.[51]

3.1. PS metal nanocomposites

The polymer-metal nanocomposites are user-friendly, effective, and environmentally safe. They are utilized for purifying water contaminated with organic azo dyes.[64]

3.1.1. Iron oxide NPs. A combination of sulfonated waste polystyrene and iron oxide nanoparticles (SWPS/FeO-NPs) to enhance the reduction process that breaks down indigo carmine dye. The best results are achieved when the pH is close to its natural state. The nanoparticles, which have an average diameter of 25.5 nm and a quasi-spherical morphology, are created by combining Fe°, Fe^{2+}, and Fe^{3+} with green tea extract.[57] A highly effective method for removing Congo red (CR) dye from solutions has been developed using sulfonated polystyrene/magnetite nanocomposites (SPS/MNPs). The MNPs were synthesized through the co-precipitation method and exhibit a spherical crystalline morphology along with superparamagnetic properties, with an average size of 5 nm. Al-Sabagh *et al.* (2018) demonstrated that recycled commercial polystyrene can be sulfonated under mild conditions to enhance its surface functionalities.[58] This process can promote the synthesis of composites by facilitating interactions between surface functional groups and nanoparticles. Using a method involving bifunctional adsorption and degradation, rhodamine B was effectively removed using hollow mesoporous magnetite that is coated with polystyrene. The successful synthesis of hollow mesoporous magnetite (HMM) was achieved through *in situ* magnetite precipitation and oxidation techniques applied to polystyrene substrates. These synthetic HMM spheres exhibit a hollow core with a diameter of 230 nm, and their overall particle size ranges between 320 and 350 nm. According to Abadi *et al.* (2022), the pore volume of HMM is 0.63 cm^3 g^{-1}, and its surface area is 132.0 m^2 g^{-1}.[53]

A recent study investigated a nanocomposite made from ferric oxide and polystyrene–alginate, designed to remove malachite green dye from water. Alginate, a widely studied biopolymer derived from brown algae, is used as a sorbent for pollutant removal due to its high adsorption capacity, low cost, non-toxicity, biocompatibility, and excellent hydrophilicity. The carboxylate groups in alginate attract the ammonium groups of cationic dyes through electrostatic interactions, enhancing its adsorption capability. This process improves the adsorption of cationic dyes when using immobilized adsorbents.[54]

The process involved removing the poly aromatic hydrocarbon pollutant (PAH) ethyl naphthalene from effluent in the petroleum industry, commonly known as produced water (PW). Using 2-azobisisobutyronitrile as an initiator, a simple and cost-effective method called *in situ* bulk radical polymerization was employed to synthesize magnetically superhydrophobic monolithic core–shell polystyrene. According to Hosny *et al.* (2023), this technology has the potential to enhance the treatment of organic pollutants in wastewater, which may lead to increased reusability of the water.[52]

Magnetic polymers derived from gel-type hypercrosslinked styrene copolymers exhibit optical transparency and feature a "micro-meso" porous structure. This includes pores as large as 6 nm and a specific surface area of 560 m^2 g^{-1}. A matrix of porous polymers was created using the industrial adsorbents Macronet and Amberlite, along with the synthesized hypercrosslinked styrene–divinylbenzene copolymer. The porous morphology of the magnetic sorbents showed a specific surface area of 1400 m^2 g^{-1} and a micropore volume (with pore sizes smaller than 3 nm) of up to 0.6 cm^3 g^{-1}, highlighting the highly developed pore system of the composites. The application of magnetic materials for the adsorption of various petrochemicals such as chlorinated hydrocarbons, aliphatic and aromatic compounds, and potentially harmful alcohols and ethers offers a promising method for magnetic separation from mineral or aqueous solutions.[56]

Table 2 Polystyrene nano-composites

Starting/nano additive	Synthesis conditions	Pollutant	Adsorption conditions	Performance efficiency	References
(I) PS metal NP					
Magnetic Fe_3O_4 NPs	Prepare magnetic Fe_3O_4 NPs *via* chemical co-precipitation. Then, use *in situ* bulk radical polymerization to create porous polystyrene (PS) monoliths, mixing them with the Fe_3O_4 NPs and sonicating for 30 minutes	Poly aromatic hydrocarbon pollutants (PAHs): ethyl naphthalene	In fixed-bed column Flow rate 2.5 mL min^{-1} Bed height 9 cm Ci 50 mg L^{-1}	PAHs-Q_{Max} 46.9 mg g^{-1} Reusability: 4 cycles Yoon–Nelson model	52
Magnetite (Fe_3O_4) NPs	A hollow mesoporous magnetite (HMM) prepared by mixing ethylene glycol, PS, $FeCl_2 \cdot 4H_2O$, KNO_3, and hexamethylene tetramine (HETM) the solution heated to 80 °C under sonication for 3 h to form the coated PS	Rhodamine-B (RhB) dye	HMM loading 0.8 wt% Ci 50 mg per L pH 6 Temp. 50 °C Time 240 min	RhB-R 99.7% Modified Langmuir Pseudo-second-order	53
Magnetite (Fe_3O_4) NPs	Addition of dispersed Fe_3O_4 to dissolved PS solution for 2 h followed by mixing with sodium alginate for 4 h, then addition into a mixture of calcium chloride and ferrous sulfate for 2 h	Cationic malachite green (MG) dye	Ci 20 mg per L pH 7 Dose 500 mg L^{-1} Time 20 min	MG-Q_{Max} 90.81 mg g^{-1} Langmuir Pseudo second-order	54
Magnetic activated carbon (MAC)	Iron(III) acetylacetonate ($Fe(acac)_3$) was added to a mixture of ethyl acetate and EPS, followed by chemical activation with anhydrous potassium hydroxide (KOH). The material was then milled at 800 °C for 1 h	Phenol (ph) Methylene blue (MB) Indigo carmine (IC)	Dose 0.75 g per L pH 3, 7, and 9 Temp. 298 K Time 24 h	Q_{Max} (mg g^{-1}) IC 623.2 at pH 3 Ph 115.7 at pH 7 MB 281.0 at pH 9 Reusability: 5 cycles Double-layer model (DLM) Pseudo-second-order	55
Iron oxides NPs	The immobilization of iron oxides into the pores of hyper-crosslinked PS sorbents *via* chemical precipitation. Using commercial porous polymer matrix: (Macronet and Amberlite)	Organic solvents Ethanol Acetone Toluene Heptane Dichloro-ethane Ethyl acetate Dioxane	Under static conditions: (0.1 g) sorbent loaded in grid stainless steel containers (D = 15 mm, H = 8 mm) Solvent vol 25 mL Temp. RT Time 24 h	Volume of the condensed adsorbate Range 0.48–0.91 through different organic solvents	56
Iron oxide NPs	SWPS added to $FeCl_2$, green tea solution and stirred for 60 min	Organic pollutant: Indigo carmine (IC) dye	Dose 6 g L^{-1} Ci 100 mg per L pH 3.2 Time 60 min	Sulfonation degree 23.5% IEC 1.2 meq g^{-1} IC-R 86.7%	57

Table 2 (*Contd.*)

Starting/nano additive	Synthesis conditions	Pollutant	Adsorption conditions	Performance efficiency	References
Magnetite (Fe_3O_4) NPs	The suspended magnetite (MNP) added to the dissolved SPS during stirring for 1 h. and the polymer nanocomposite precipitated	Congo red (CR) dye	Dose 0.4 g L^{-1} Ci 50 ppm pH 7 Temp. RT Time 60 min	CR-Q_{Max} 76.29 mg g^{-1} Langmuir Pseudo second order	58
Silver NPs	Introduction of silver ammonia solution to sulphonated PS for 3 h at 60 °C	Methylene blue (MB) dye	Mass of microspheres 1 mg DW 0.5 mL MB 2 mL Ci 0.15 mM	Surface area 68.51 m^2 g^{-1} Degradation 97.12% Reusability: 5 cycles	59
Silver NPs	Nanocomposite preparation by a mixture of sodium citrate and $AgNO_3$ added to PS commercial (D201) for 24 h at 50 °C	Iodide	Dose 0.1 g L^{-1} Ci 100 mg per L pH 2 Temp. 25 °C	Iodide-Qe 802 mg g^{-1} Langmuir Pseudo-first-order	60
Silver NPs	Immobilization of Ag NPs on PS was achieved by submerging the material in a mixture of PVP, glucose, silver ammonia solution, and ethanol, followed by chemical plating pretreatments at 20 °C for 60 min	Methylene blue (MB) dye	Sodium borohydride (NaBH4) as a reducing agent in MB reduction $NaBH_4$-Ci 30 mM MB-Ci 0.05 mM Dose 1 g L^{-1}	Reduction: 90% Reusability: 5 cycles Pseudo-first-order	61
Cobalt and aluminum hydroxides NPs	Polystyrene/chitosan is polymerized and then modified with metal hydroxide nanoparticles ($CoCl_2$ and $Al(NO_3)_3$) *via* co-chemical precipitation for 10 minutes	Cadmium (Cd) ions	Dose 0.5 g L^{-1} Ci 50 ppm pH 5 Temp. RT Time 60 min	Cd-Q_{Max} 112.36 mg g^{-1} Reusability: 5 cycles Langmuir Pseudo-second-order	62
Cobalt hydroxide NPs	The synthesis of polystyrene using high-internal phase emulsion (HIPE) polymerization, then incorporated with alkali cobalt particles for 15 min	Methylene blue (MB) dye	Ci (mg g^{-1}) 10–100 | MB 40–200 | iron pH 6.5 | MB 2 | iron Time 180 min	MB-Qe 75.2 mg g^{-1} Fe(III)-Qe 112.3 mg g^{-1} Reusability: 3 cycles Langmuir	63
		Iron (Fe(III)) ions	Temp 25 °C	Pseudo second order	
Cobalt ferrite magnetic NPs	The co-precipitation process for cobalt ferrite magnetic NPs involves dissolving cobaltous nitrate ($Co(NO_3)_2$) and ferric nitrate ($Fe(NO_3)_3$) before adding them to an alkaline medium	Calcon dye	Dose: 5 g L^{-1} Ci 50 ppm pH: natural Temp. RT Time 240 min	Dye degradation from 515–260 nm Absorbance peaks: 515 nm (red), shifted to (536 and 565 nm) after 5 min Reusability: 3 cycles	64
Copper and Nickle NPs	CMC-PSIS films prepared by dissolving polyisoprene-*block*-polystyrene (PSIS), and dispersing CMC in the mixture. The films are immersed in a $Cu(NO_3)_2 \cdot 5H_2O$ and $Ni(NO_3)_2$ solution for 24 hours and then treated with sodium borohydride ($NaBH_4$) to create zero-valent Cu and Ni nanoparticles	4 pollutants 4-Nitrophenol (4NP) Methylene blue (MB) Rhodamine B (RB) Methyl orange (MO)	Dose 5 g L^{-1} Time 6–4 min Ci 0.05 mM | MB 0.1 mM | 4NP	Degradation 97.7% among all 3 dyes Reduction for 4NP 91% Highest rate for reusability: single or second cycle Zero-order kinetics	65

Table 2 (*Contd.*)

Starting/nano additive	Synthesis conditions	Pollutant	Adsorption conditions	Performance efficiency	References
Titanium oxides (TiO) NPs	Ti was loaded to PS beads by stirring for 24 h and precipitated as Ti hydroxide onto the inner surface of PS followed by thermal treatment at 338 K for 12 h	Phosphate (PO_4^{3-})	Batch Dose 0.5 g L^{-1} Ci 10 mg per L pH 6.5–7.5 Temp. 298 K Time 12 h Fixed-bed column Ti-PS or PS beads Temp. 298K. Ci 2 mg L^{-1}	PO_4^{3-} – Q_{Max} 44.14 mg g^{-1} of batch test Reusability: 5 cycles of the column test Double Langmuir Pseudo-first-order, and Intraparticle diffusion model (IDM)	66
Nickel hydroxide NPs	Addition of $NiCl_2$ aqueous solution to PS then after 15 min alkaline solution was added till pH 10–11 for complete precipitation	Methylene blue (MB) dye Fe(III)	Dose 1 g L^{-1} Ci MB 40 mg L^{-1} Fe^{3+} 100 mg per L pH 6.5 Temp. 23 °C Time 150 min	MB-Q_{Max} 32.73 mg g^{-1} Fe-Q_{Max} 58.24 mg g^{-1} Freundlich Pseudo-first-order	67
Zinc oxide NPs	Aqueous dispersion of thermally linking styrene–acrylic copolymer, then introduction of zinc oxide NP under stirring, for 5 min	Methylene blue (MB) dye	Dose 1.2 g L^{-1} Ci 300 ppm pH 6 Time 24 h	MB-Qe 150 mg g^{-1}	68
Chromium metal organic frameworks (MOF-cr)	(MOF-Cr) was prepared by mixing of chromium(III) nitrate, and 2 acids for 20 min at RT, after that, hydrothermal synthesis (220 °C for 8 h). Finally, adding MOF-Cr into polystyrene waste (PSW) solution for 4 h, then electrospinning	Cationic crystal violet (CV) dye	Dose 1 g L^{-1} Ci 100 mg per L pH 10 Temp. 298 K Time 24 h	pH_{PZC} 6 CV-Q_{Max} 354.49 mg g^{-1} Reusability: 7 cycles Langmuir Pseudo-second-order	69
(II) PS silica					
Silica NPs	Silica nanoparticles (NPs) were coated with a polystyrene (PS) layer through high internal phase emulsion (HIPE) polymerization. The emulsion was then heated at 60 °C for 12 hours, producing porous core–shell structures	Methylene blue (MB) dye	Dose 5 g L^{-1} Ci 100 mg L^{-1} Temp. RT Time 60 min pH 6	MB-Q_{Max} 23.1 mg g^{-1} Reusability: 5 cycles Langmuir Pseudo-second-order	70
Octavinyl–polyhedral oligomeric silsesquioxane (OV-POSS)	Lignin and OV-POSS were added to the PS solution with stirring, then cooling the temperature from 115 to 20 °C	Oil or organic solvent water separation Vegetable oil, chloroform	Adsorbent Mass 0.8 g Ci 5 g/100 mL PH 7 Temp. 25 °C Time 30 min	Oil-Qe 21–33 g g^{-1} R 90% Reusability: 10 cycles Langmuir Pseudo-second-order	71

Table 2 (*Contd.*)

Starting/nano additive	Synthesis conditions	Pollutant	Adsorption conditions	Performance efficiency	References
Octadecyltrichlorosilane (OTS)	Preparation of nano silica (SiO_2) from dye diatomite filter aid waste (DDW), then silanize it (OTS) to form hydrophobic nanosilica ($hSiO_2$) by solution impregnation. (PS/hSiO2) prepared by electrospinning, showing superhydrophobicity composite	Oil-water separation (transformer oil)	Dose 0.4 g L^{-1} Time 20 min	Oil-Q_{Max} 136.4 g g^{-1} Reusability: 5 cycles	72
Silica (SiO_2) NPs	The nanocomposite polyurethane-SiO_2-poly (styrene-co-oleic acid) prepared *via in situ* free radical polymerization. Fabricated by (dip coating) coating the (PU) sponges with synthesized organic–inorganic NP by immersion method and polydimethylsiloxane (PDMS) as a coupling agent	Oil–water separation (motor oil)	Oils separately added to containers containing 50 mL of water, the composite introduced into each mixture Temp. RT Time 5 min	Oil-Q_{Max} 60.83 g g^{-1} Reusability: 10 cycles Langmuir Pseudo-second-order	73
Silicon dioxide (SiO_2) NPs	PS dissolving followed by sulfonation, then PS sulfonic acid was loaded with quartz (or silica) adsorbents prepared by the sequential incipient wetness impregnation method	Methylene blue (MB) dye	Ci 25–100 mg per L pH 7	MB-Q_{Max} 434 mg g^{-1} Reusability: 4 cycles	74
(III) PS hybrid NPs					
Magnetite, and silica	The magnetic nanospheres prepared by polymerization of styrene in presence of Fe_3O_4–SiO_2, dodecyl sulfate, divinylbenzene, and benzoyl peroxide with raising temperature for each addition step from 35, 45, finally 80 C after all additives for 2 h	Organochlorine pesticide residues in food	Dose 10 mg Ci 0–20 mg per L pH 6 Time 1 h	Pesticide-Qe 16.67–20.53 mg g^{-1} Reusability: 6 cycles Recovery %: 74.7–93.7 Pseudo-second-order	75
Iron oxide (IO), and silica	Firstly steps, iron oxide NP (IONP) synthesized by the solvothermal method, then silica-coated-IONP was prepared, and after that functionalization of SiO_2-IONP with an azobisisobutyronitrile. (AIBN) initiator using a bromine-functionalized silane	Oil spills on water: low-density (diesel)	Ci 5 g of oil in 500 mL of water	Oil-Qe 3–5 g oil/g absorbent	76

Table 2 (*Contd.*)

Starting/nano additive	Synthesis conditions	Pollutant	Adsorption conditions	Performance efficiency	References
			Mass 20 mg Temp. 23 °C		
	Finally, carried out reverse atom transfer radical polymerization (ATRP) and surface initiated ATRP (SI-ATRP) in the same reactor using the same catalyst complex to grow polystyrene grafts on the surface of Br-SiO_2-IONP	High-density (bitumen in toluene)	Time 5 min		
Multi-walled carbon nanotube (MWCNTs), and magnetite	MWCNTs functionalized by oxidation with strong acids HNO_3, H_2SO_4, and H_2O_2. Then, preparation of magnetite/MWCNTs nanocomposites then dissolved polystyrene was added with sonication for a 3 h, and magnetic stirrer for 24 h at 40 °C	Oil pollutant: toluene	Dose 1–6 mg Ci 200 mg per L pH 2–10 (5) Temp. 35 °C Time 60 min	R 62% Toluene-Qe 1113 mg g^{-1} Langmuir Pseudo-second order	77

In a traditional two-step process, recycled polystyrene foams are converted into magnetic activated carbon (MAC). The synthesized carbonaceous magnetic materials exhibit a specific surface area of 672 m^2 g^{-1} and a total pore volume of 0.35 cm^3 g^{-1}. Additionally, these materials contain nanometric phases of Fe°, Fe_3C, and Fe_3O_4. As a result of their exceptional electrical, chemical, and textural properties, magnetically collected and regenerated MAC has been successfully utilized to create both organic pollutant adsorbents and redox supercapacitor electrodes.[55]

Researchers have finally developed core–shell magnetic nanoparticle polystyrene nanocomposites that incorporate iron oxide and cobalt. These advanced materials are ideal for high-performance applications that require elevated temperatures. They increase the surface temperature, which facilitates the melting and repair of large cracks.[78]

3.1.2. Silver NPs. Polystyrene silver nanocomposite microspheres developed by Liu *et al.* (2022) and H. Xu *et al.* (2023) have been utilized for the catalytic reduction of organic dyes, specifically methylene blue (MB). A two-step seed-swelling polymerization technique was employed to create polystyrene–divinylbenzene mesoporous microspheres and their composites with silver nanoparticles (Ag NPs). The composite microspheres containing sulfonic acid exhibited different degradation rates for methylene blue than those containing silver nanoparticles. The study also investigated how various swelling agents influenced the shape and architecture of the mesoporous microspheres. Degradation experiments demonstrated that the introduction of hydrophilic sulfonic acid groups facilitated faster adsorption of MB by the microspheres. Furthermore, the presence of silver nanoparticles significantly enhanced the degradation rate of MB by 90–97%, as they can effectively catalyze the reduction of MB.[59]

Dispersion polymerization produces monodispersed PS microspheres. A water-based modified chemical plating method was used to synthesize PS/Ag composite microspheres that contain silver nanoparticles. The catalyst and reducing agent for MB reduction were the PS/Ag composite microspheres and sodium borohydride (NaBH4).[61] A recent study discovered that Ag-D201, a complex created by grafting silver nanoparticles (Ag NPs) onto D201 resins, effectively removes iodide ions (I^-) from water. The presence of dissolved oxygen helps the Ag NPs facilitate the oxidation of iodide ions. According to L. Li *et al.* (2023), Ag-D201 adsorbents exhibit a strong preference for I^- even in the presence of competing anions such as sulfate, nitrate, bicarbonate, and chloride.[60] Shape-memory polystyrene sheets doped with silver nanoparticles (AgNPs) serve as a substrate for surface-enhanced Raman scattering (SERS), allowing for the visualization of heat-induced hot spots. The gaps between the particles in the AgNP-decorated shape-memory polystyrene (Ag-SMP) substrates were optimized by adjusting the formulation and reduction technique to enhance hot spot effects during thermal shrinkage.[79]

3.1.3. Cobalt NPs. The polystyrene/chitosan for water cadmium removal procedure was enhanced by adding cobalt ($CoCl_2$) and aluminium (Al $(NO3)_3$) metal hydroxide nanoparticles. Polystyrene and fungal chitosan formed a narrowly

mesoporous material. In contrast, sub-driven nanocomposite material was microporous. The polystyrene/fungal chitosan (P-AFC) structure has a surface area of 57.0 m^2 g^{-1}, compared to 36.9 m^2 g^{-1} for the fungal chitosan–polystyrene–Co nanocomposites (FCPNC) structure. Chitosan, due to its chemical structure may remove anions or cations, depending on the pollutants. Chitosan's limited specific surface area, low mechanical strength, lack of porosity, and excess of functional groups limit its usage in water treatment. Using nanoparticles to synthesize new sorbents that improve chitosan's mechanical properties, solubility, and adsorption: nano-sized adsorbents function well due to their high specific surface area and absence of intra-particle diffusion interference.[62]

A polymer-metal nanocomposite that degrades Calcon dye by combining sulfonated waste polystyrene (SWPS) with cobalt ferrite magnetic nanoparticles ($CoFe_2O_4$-MNp) in varying concentrations. A decrease in average particle size from 27.5 to 1.1 nm was observed with an increase in MNp loading; subsequently, their effectiveness in degrading azo dye was evaluated. Degradation caused by the small size of SWPS/MNp particles. MNp $CoFe_2O_4$ has several applications due to its excellent magnetic characteristics. The effectiveness of the design intended for degrading dye from water-based solutions is hindered by solution aggregation and limited surface accessibility. The agglomeration of $CoFe_2O_4$ prevented through surface modification using SWPS. This method modifies the physicochemical characteristics of nanoparticles by manipulating their size and shape.[64]

Other research showed, *via* surface property measurements, that the enhanced specific surface area of cobalt hydroxide nanoparticles doped in PS functions as an adsorbent for the removal of dyes and heavy metals from wastewater.[63]

3.1.4. Copper NPs. Copper and nickel nanoparticles were synthesized and incorporated into a carboxymethyl cellulose–polystyrene derivative (CMC-PSIS) solid substrate, which was then molded into films. Both types of nanoparticles acted as dip catalysts, with sodium borohydride ($NaBH_4$) used as a reducing agent to reduce 4-nitrophenol (4NP) or to degrade cationic dyes. The nanofibrous structure and the presence of –OH groups in cellulose make it an ideal matrix for hosting metal nanoparticles.

For instance, PSIS, which stands for polystyrene-*block*-polyisoprene-*block*-polystyrene, is a block copolymer that exhibits a range of physical characteristics, including hydrophobicity and elasticity. It also possesses outstanding mechanical strength. By dispersing metal nanoparticles within bacterial cellulose, nanocomposites with both magnetic and elastic properties are created.[65]

The addition of copper particles and a lead/tin solder alloy enhances the electrical conductivity of polystyrene. For optimal conductivity, the application of flux is essential. The "bulk soldering" procedure is employed to combine polystyrene, molten solder, and copper particles to create conductive thermoplastic polymer composites. It is important to remove the oxide coating from the copper particles before the solder can effectively wet them.[80] Micelles, which have particle diameters ranging from 10 to 40 nm, enhance thermal stability and reduce clumping in composites made of copper nanoparticles and polystyrene (CuNPs/PS). Compared to pure polystyrene, the polystyrene in the CuNPs/PS composite exhibits a lower polydispersity index and a higher molecular weight.[81]

3.1.5. Titanium NPs. Polystyrene and titanium dioxide (TiO_2) nanoparticles chemically bond to create composites that achieve high coating efficiency while displaying unique electrical and visual characteristics. Recent studies have shown that macroporous polystyrene beads (NS) functionalized with quaternary ammonium groups possess a specific pore size along with a high density of positively charged groups connected to the polystyrene matrix. The nanocomposite Ti-NS, which consists of these macroporous structures immobilized with titanium oxides, is designed to enhance phosphate removal from wastewater. Additionally, it is important to consider how the presence of competing ions (SO_4^{2-}, NO_3^-, and Cl^-) affects phosphate removal.[66]

The study conducted by W. Wang *et al.* (2013) investigates how ultraviolet light affects shape memory in titanium oxide-polystyrene (TiO-SMPS) nanocomposites. This nanocomposite can absorb light energy, resulting in physical or chemical interactions either within the molecules or between them. The TiO-SMPS composite has enhanced optical absorption, making it an ideal candidate for applications in biomedicine, actuators, and the automotive industry.[82]

3.1.6. Others. The project involves the incorporation of chromium terephthalate metal–organic frameworks (MOF-Cr) and the upcycling of polystyrene foam waste (PSW) through electrospinning. The goal is to create a nanofiber composite adsorbent capable of capturing hazardous cationic organic dyes, specifically crystal violet. Nanofibers produced from polymers with limited functional groups, such as polystyrene, require modification to enhance their adsorption capabilities. Metal–organic frameworks (MOFs) can significantly improve the adsorption properties of these nanofibers due to their high surface area and multiple adsorption sites. MOFs are effective at absorbing pollutants and organic dyes. However, after the adsorption process, powdered MOFs can be challenging to separate from aqueous solutions, leading to potential secondary contamination. To address issues related to the separation, reuse, handling, and difficulties associated with powdered MOFs, this study will explore the possibility of attaching MOFs directly to the nanofibers.[69]

The study focuses on using composites of nickel hydroxide and polystyrene to adsorb methylene blue and iron(III) from water. Hydroxides and metal oxides are known for their numerous active sites and high specific surface areas. However, their large surface area relative to their volume can lead to clumping. This issue can be addressed by creating hybrid polymeric/inorganic materials that combine polymers with metal oxides and hydroxides.[67]

A thermally coupled styrene-acrylic copolymer partially esterified with melamine resin and incorporating 20 nm ZnO nanoparticles as a filler, formed polymer nanocomposite films in water. The presence of extra chains in the styrene-acrylic polymer, along with a crosslinking agent and the Nano ZnO, enhanced intermolecular cross-linking while reducing swelling

in both water and benzene. In these polymer nanocomposites, zinc oxide nanoparticles serve as bactericides and active sites. Active sites in ZnO are created by oxygen vacancies, oxygen interstitials, and zinc interstitials, which help prevent electron–hole recombination. Additionally, the three-dimensional structure of ZnO nanoparticles within the polymer film improves mechanical properties and stabilizes the nanoparticles.[68]

Lead was removed and reinforced using polystyrene, which was supported by zirconium phosphate nanoparticles. The dispersion of Nano-ZrP is significantly improved by the presence of charged functional groups, such as $-SO_3$ and $-CH_2N^+(CH_3)_3$, compared to the neutral CL group. In addition to potential specific interactions with selected contaminants, the superior performance of inorganic nanoparticles can be attributed to their higher surface-to-volume ratio and increased number of active sites compared to bulk materials.[83]

3.2. PS clay nanocomposites

In addition to being novel and cost-effective, polymer nanocomposite raw materials derived from clay minerals possess a layered structure, a high aspect ratio, exceptional in-plane strength and stiffness, and versatile intercalation chemistry. Nanoclays, including kaolinite, bentonite, hectorite, and montmorillonite, are used to enhance the mechanical properties and performance of polymers. Clay-polymer nanocomposites can be exfoliated, intercalated, or phase-separated, offering excellent deformation, biodegradability, and chemical resistance, while also eliminating contaminants. Compared to their individual components, clay-polymer nanocomposites (CPNs) demonstrate superior performance in water treatment and adsorption. Moreover, CPNs renew more effectively than conventional clay materials. These composites can be made from various polymers, including polyesters, chitosan, polyvinyl chloride (PVC), PP, epoxies, PS, and PU. They improve the mechanical characteristics, flame retardance, solvent resistance, thermal stability, and barrier properties of affordable nanostructured polymeric materials, such as polystyrene. However, the ability of clay-polystyrene nanocomposites, a specific type of CPN, to remove water impurities has not been thoroughly investigated.[34,84,85]

Shape memory nanocomposites were developed using chemically cross-linked PS copolymers combined with various nano fillers, such as alumina, silica, and clay. Compared to unreinforced PS, these nanocomposites exhibit enhanced thermal and mechanical properties, including shape memory characteristics. Notably, heat-treated nano clay provided the most significant improvement in strength, while composites containing clay achieved the highest storage modulus and optimal energy absorption capacity.[86]

Organoclays possess a layered structure but have a low surface area, poor hydrophilic sites, and face challenges such as clay particle aggregation and mineral impurities when untreated. These characteristics can be improved through acid treatments and other methods. Organoclays have a wide range of applications, including serving as fillers in membrane technology to enhance barrier performance and in various polymer technologies. The combination of organoclay (OC) with PS or PVC demonstrates good miscibility. The cation exchange method employed to produce organoclay uses cetylpyridinium chloride as the cationic surfactant. The miscibility of PS and PVC polymers is further enhanced by the multiple layers of exfoliated organoclay.[87]

Nano clay and polystyrene nanocomposites represent some of the most exciting and rapidly evolving fields in polymer science and technology. These polystyrene/clay composites serve as effective adsorbents for removing heavy metals, such as lead ions, from wastewater due to their porous structure and high surface area.[88] A recent study highlighted that ceramic membranes, which are hybrid membranes composed of kaolin and expanded polystyrene, are effective in removing methylene blue from water. Heating the membranes to 1000 °C deteriorated the polystyrene, allowing the clay matrix to expand its surface area and create pores.[89]

Nano zeolites (NZ), characterized by a uniform crystal size of 100 nm, are highly effective proton conductors. This effectiveness is due to their larger outer surface areas, smaller channels, and shorter diffusion path lengths compared to micro zeolites. The high silica content and solid acidity of NZs further enhance the proton conductivity of hybrid materials. At elevated temperatures, the functionalized nanocomposite exhibits a proton conductivity of 1×10^{-3} S cm^{-1}, while also demonstrating hydrophilic properties, chemical stability, and impressive mechanical strength.

According to El Mansoub *et al.* (2025), sulfonated polystyrene is incorporated into inorganic and organic composites by using NZ as a catalyst in a microwave-assisted process. The effectiveness of these resins in removing cationic dyes, such as methylene blue and safranin T, from synthetic solutions has been evaluated, revealing high absorption capacities.[90]

3.3. PS silica nanocomposites

The fascinating properties of organic–inorganic hybrid composites include catalytic, optical, mechanical, electrical, and magnetic capabilities. Among these composites, polymer/silica composites stand out due to their mechanical characteristics and morphologies. Silica is an excellent material because of its porosity, high specific surface area, malleability, and resistance. Silica fillers have several surface groups and exhibit hydrophilic properties.

There are both physical and chemical methods for modifying the surface of precipitated or colloidal silica. Polymer/silica composites have a wide range of potential applications, including enzyme immobilization, dye adsorption, coatings, catalysis, biomedicine, medicine, electronics, and the removal of harmful metal ions from wastewater. Additionally, silica is a common additive to PS, which is a widely used filler in both inorganic–organic and organic–organic composites due to its many beneficial qualities.[35,91]

Hollow mesoporous silica microspheres (HMSMs) are a distinct type of nanomaterial characterized by their hollow structure and mesoporous features, with pore sizes ranging

from 2 to 50 nm. These microspheres offer several advantages, including a high specific surface area, significant pore volume, tailored pore sizes, low density, lightweight properties, chemical stability, and controlled release capabilities. HMSMs are utilized in various applications such as drug delivery, catalysis, adsorption, and environmental remediation. They are typically produced using polystyrene microspheres (PSMs) as templates, cetyltrimethyl ammonium bromide (CTAB) as a surfactant and pore-forming agent, ammonia solution as an alkaline catalyst, and tetraethyl orthosilicate (TEOS) as a silica source. The resulting HMSMs have an average diameter of 336.33 nm and a shell thickness of 14.52 nm, exhibiting high dispersibility and uniformity. Increasing the amount of CTAB can enhance the uniformity and completeness of the SiO_2 coating on the PSM template.[92]

The structure, thermal behavior, and fabrication of polycrystalline silicon (Si) and PS nanocomposites were examined. In these nanocomposites, the polymer matrix contains clusters of silicon nanoparticles. The presence of silicon nanoparticles, particularly those measuring 50 nanometers, increases the thermal breakdown temperature of polystyrene. Additionally, when silicon nanoparticles are evenly distributed throughout the polymer matrix, they create a heat barrier. The movement of polymer macromolecules is primarily limited by adsorption occurring on the porous surface of the silicon.[93] Silica support is utilized to immobilize azomethine in polystyrene/silica composites. Alternative names for functionalized polystyrene include $PSNO_2$, PSH, PSCl, and $PSCH_3$. The APSH-Si composite shows significant potential for industrial applications due to its superior surface roughness and enhanced heat stability, which result from the interaction between silica and the polymer matrix.[91]

The recently introduced combination of polystyrene and silica nanoparticles has demonstrated promising adsorption capabilities for methylene blue (MB) dyes, thanks to its advantageous porous structure. To enhance the effectiveness of these composites in removing dye species, a layer of highly porous polystyrene was applied to cover the polar silica nanoparticles. The pores in the polystyrene allow dye molecules to interact with the silicon oxide particles, providing selectivity for the organic components of the MB dye.[70] This process allows for the recycling of expanded polystyrene by synthesizing polystyrene sulfonic acid (PSSA). Composites of polystyrene sulfonic acid and silicon dioxide are utilized as solid adsorbents to remove organic dyes from water. Fig. 4 displays the $PSSA/SiO_2$ composite structure, which illustrates how the sulfonated polystyrene chains and silica nanoparticles work together to improve the adsorption efficacy. Sulfonic acid groups ($-SO_3H$) attached to polystyrene backbones create negatively charged active sites where cationic pollutants can interact through electrostatic interaction and ion-exchange processes. Hydrophilicity, surface complexation with metal ions, and hydrogen bonding are all enhanced by the addition of silica particles, which also increases the quantity of surface hydroxyl groups (–Si–OH). Because of the increased surface area and the fact that the polymer chains do not clump as a result of the dispersion of SiO_2 within the matrix, the adsorption sites are also more

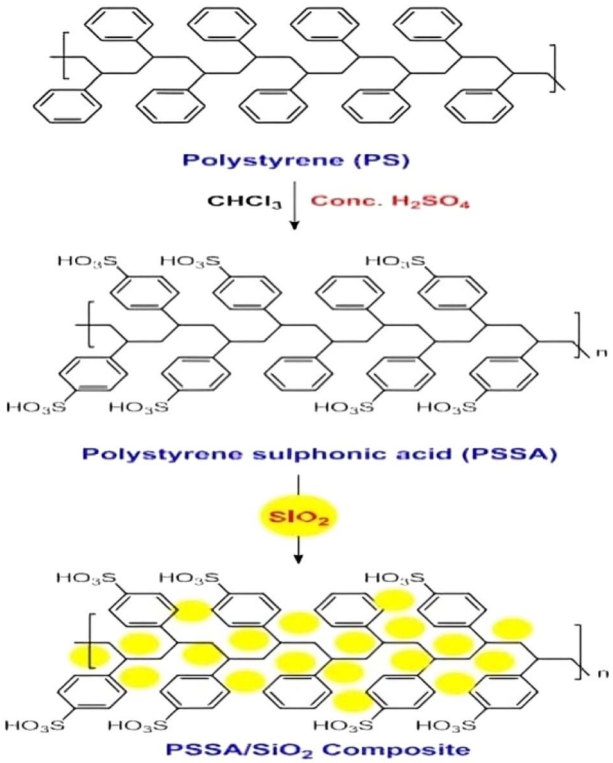

Fig. 4 The $PSSA/SiO_2$ composite structure is presented schematically as an interaction between sulfonated polystyrene chains and silica nanoparticles. The sulfonic acid groups and surface hydroxyl groups of the silica contribute to electrostatic interaction, ion exchange, hydrogen bonding, and improved accessibility of the adsorption sites, reproduced from an open access source.[74] [R. Abouzeid, H. Dardeer, M. Mahgoub, and A. Abdelkader, 2021], licensed under CC BY.

accessible. This organic–inorganic hybrid structure outperforms pure sulfonated polystyrene materials in terms of mechanical stability, swelling behaviour, and adsorption efficiency. The impregnation process creates $PSSA/SiO_2$ composites using quartz in three different concentrations: 5%, 10%, and 20%. Composites made with PSSA exhibit enhanced thermal stability, improved surface morphology, and increased crystallinity.[74]

Monoliths made from polystyrene, lignin, and nanoparticles of OV-POSS (a rigid inorganic silica cage structure) were developed for wastewater treatment through a process called thermal-induced phase separation (TIPS). Lignin serves as an effective filler or reinforcement in thermoplastic polymers, creating a hybrid system with improved properties. The addition of OV-POSS enhanced the compatibility of the matrix system and improved the dispersion of lignin. The thermal properties of the blend were also improved after incorporating POSS into the monolith. Additionally, the surface characteristics of the monolith were enhanced, increasing its oleophilicity and altering the water contact angle. With a separation efficiency exceeding 90%, this blend effectively and selectively absorbs organic liquids and oils from water mixtures.[71] Polymer composites that include polar hydrophilic silicon nanoparticles, often referred to as white carbon black, exhibit lower thermal heat capacity and improved dispersion stability when

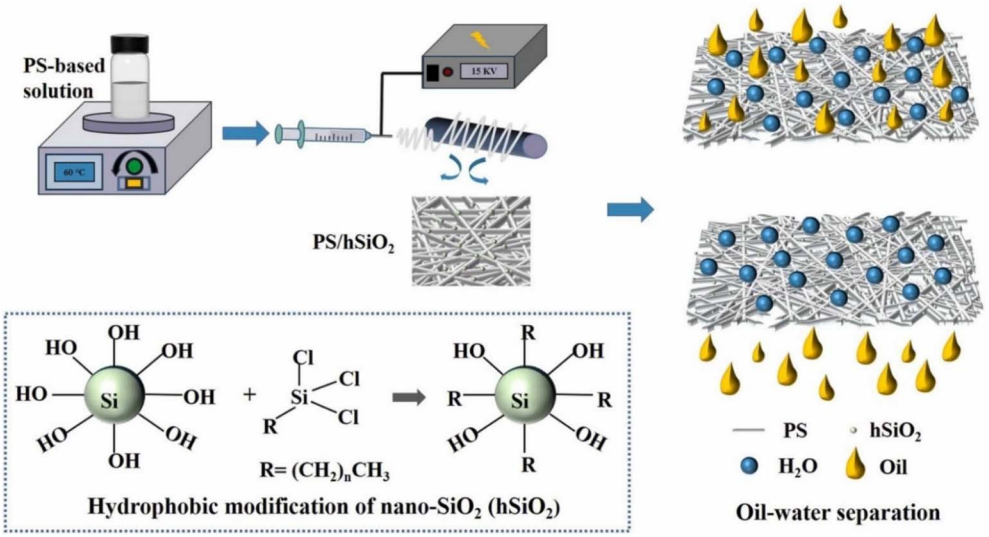

Fig. 5 This is a schematic showing the hydrophobic modification of nano-SiO_2 by grafting silane onto electrospun polystyrene fibers, and the subsequent mechanism of selective oil–water separation by means of decreased surface energy, enhanced surface roughness, and the formation of structured porous structures. Reproduced from[72] with permission from [Elsevier] [Zhihui Dong,Nan Qu,Qiushi Jiang, Tong Zhang, Zhaolian Han, Jiapeng Li, Ruiqi Zhang, Zhiqiang Cheng, *Journal of Environmental Chemical Engineering*, **12**(2024)112690], copyright 2024.

modified with silanes. An effective oil absorption material is created through the synthesis of electrospun nanosilica composites made from polystyrene and silane. These composites can absorb oils up to 136 times their weight, making them exceptional oil absorbents. Hydrophobic nano-SiO_2 modified polystyrene composite fibers and their use in oil–water separation are shown in Fig. 5. At first, hydrophilic silica is transformed into hydrophobic nano-SiO_2 ($hSiO_2$) by chemically modifying silica nanoparticles with surface hydroxyl groups (–Si–OH) through silane coupling processes and adding hydrophobic alkyl chains to their surfaces. The modified nanoparticles are electrospun into a fibrous structure across the polystyrene matrix, creating a homogeneous distribution. Composite fibers with hydrophobic alkyl-grafted silica have a structured micro/nano-structured interface that is highly oil-affinic and water-repellent due to increased surface roughness and decreased surface energy. The porous composite network allows oil droplets to pass through but water cannot, according to the combined effects of surface-modified silica and the hydrophobicity of polystyrene. Therefore, compared with pure polystyrene fibers, the PS/$hSiO_2$ composite membrane exhibits enhanced stability and separation efficiency.[72]

By adsorbing and polymerizing the aniline medium, the sulfonated polystyrene template particles effectively bond with the silica particles. The microgel structure enables both the aniline medium and the silica particles to expand into the polystyrene sulfonate (PSS) particle shells. This process results in the formation of silica microcapsules with customizable shell thicknesses.[94]

3.4. PS hybrid nanocomposites

Silica magnetic microspheres coated with polystyrene are utilized to estimate organochlorine pesticide residues in food. The adsorbent is made from a composite material known as Fe_3O_4-SiO_2-PS, which is created using chemical co-precipitation and polymerization cross-linking processes. This procedure involves coating magnetic microspheres with layers of polystyrene and silica. Larger particles are less likely to clump together, exhibit greater hydrophobicity, and can be more easily dispersed in solutions. This method partially addresses the issue of self-settling, which reduces the effectiveness of magnetic adsorbents, as polystyrene and water have similar densities.[75]

A stable superhydrophobic structure has been developed by immersing synthesized organic–inorganic nanoparticles in polyurethane (PU) sponges, using polydimethylsiloxane (PDMS) as a coupling agent. This method enables effective oil–water separation. The organic–inorganic nanoparticles consist of silica (SiO_2) nanoparticles that are grafted onto a copolymer made of polystyrene and oleic acid. The combination of the hydrophobic properties of polystyrene and oleic acid, along with the modified nanoparticle's ability to create surface roughness, allows the sponge to exhibit stable superhydrophobic characteristics.[73]

Polystyrene/silica and poly(styrene-co-butyl acrylate)/silica nanocomposite particles are produced using commercially available, non-functionalized silica nanoparticles through a Pickering emulsion polymerization process. Two key factors contribute to the adherence of silica nanoparticles to the growing latex particles: the ability of more hydrophobic oligomers to wet the hydrophilic silica nanoparticles, and the electrostatic interaction between the silica nanoparticles and oppositely charged oligoradicals.[95]

Magnetic polystyrene nanocomposite mixes incorporate silica-coated iron oxide nanoparticles. These hydrophobic and oleophilic magnetic polymer nanocomposites effectively

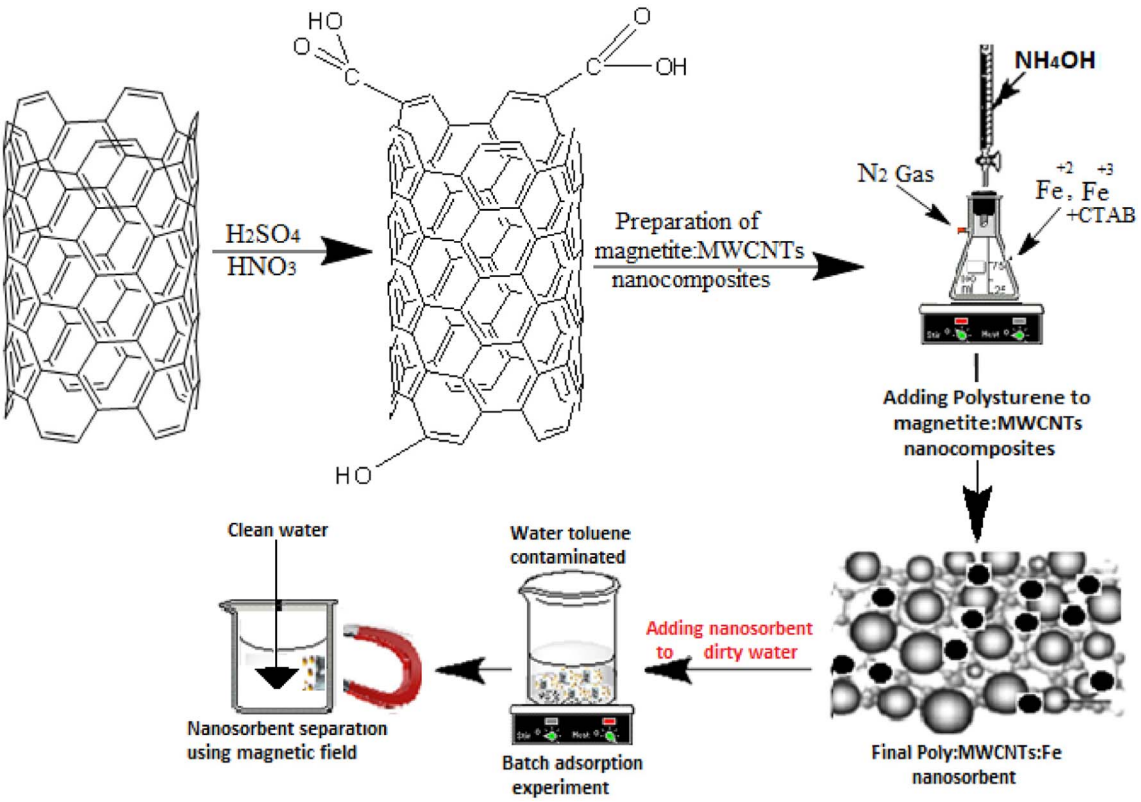

Fig. 6 Schematic of magnetic MWCNT/polystyrene nanosorbent preparation: (i) oxidative functionalisation of MWCNTs with H_2SO_4/HNO_3 to introduce oxygen-containing groups (–COOH, –OH); (ii) *in situ* deposition of Fe_3O_4 nanoparticles on functionalised MWCNT surfaces with Fe^{2+}/Fe^{3+} salts and CTAB under N_2 atmosphere; (iii) incorporation of magnetic MWCNTs into polystyrene nanosorbent. Magnetite facilitates efficient magnetic recovery after adsorption, while surface oxygen functionalities improve hydrophilicity, dispersibility, and Fe_3O_4 growth nucleation, reproduced from an open access source.[77] [T. A. Abdullah *et al.*, 2021], licensed under CC BY.

remove oil from water in a rapid manner. A new line of absorbents exhibits exceptional hydrophobicity, low density, and allows for easy magnetic separation, making them effective for recovering oil from both freshwater and saltwater spills.[76]

Polystyrene, ferric oxide, and multiwall carbon nanotube nanocomposites exhibit elevated adsorption capacity and removal efficiency for aqueous toluene absorption as shown in Fig. 6. Oxygen-containing functional groups, mainly carboxyl and hydroxyl, are introduced to multi-walled carbon nanotubes (MWCNTs) by oxidizing them with strong acids as HNO_3, H_2SO_4, and H_2O_2, increasing surface polarity and wetting while creating negatively charged sites for binding Fe^{2+}/Fe^{3+} ions. Magnetite nanoparticles form on these functionalized nanotubes through controlled base addition (NH_4OH), with cetyltrimethyl-ammonium bromide (CTAB) acting as a surfactant to prevent bulk precipitation and ensure uniform dispersion. The resulting composite sorbent, made by combining magnetite-decorated MWCNTs with polystyrene, provides adsorption sites for aromatic organics like toluene *via* π–π interactions and van der Waals forces. The polystyrene matrix enhances mechanical strength and modulates hydrophobicity, affecting uptake kinetics. The nanosorbent effectively absorbs toluene, and surface oxygen groups may facilitate secondary interactions with polar species. Post-adsorption, the composite can be easily recovered using a magnetic field.[77]

4. PS-based composites industrial-scale challenges

4.1. Approaches for copolymerization and polymerization

The three predominant *in situ* polymerization techniques for PS nanocomposites are bulk, emulsion, and suspension approaches. Mocan & Uyanik (2013) presented the outcomes of a direct comparison between *in situ* bulk and emulsion polymerization. Emulsion polymerization produced nanocomposites with enhanced thermal properties and increased clay interlayer spacings, signifying that the polymer was more efficiently intercalated into the clay galleries.[96] Conversely, emulsion polymerization necessitates a precise selection of surfactants, including sodium dodecyl sulphate (SDS) or quaternary ammonium salts, as well as initiators such as water-soluble potassium persulfate (KPS) or oil-soluble azobis-isobutyronitrile (AIBN), all of which influence the ultimate morphology, polymerization rate, and particle size.[97] Ghasemzadeh *et al.* (2014) noted that including organoclay during suspension polymerization decreased monomer conversion and increased particle size. This occurs due to the interaction between clay and the kinetics of polymerization.[98] Nair (2017) tested AIBN and benzoyl peroxide (BPO) as initiators for *in situ* PS/kaolinite synthesis; AIBN was determined to be more forgiving. Composites made *via* BPO synthesis in an

environment devoid of nitrogen had low molecular weight and conversion, in contrast to AIBN, which, when synthesized in nitrogen, exhibited much improved mechanical characteristics.[99] At low clay loadings (about 2 wt%), *in situ* polymerization yielded the most superior mechanical properties and intercalation. Nevertheless, with increased loadings, this benefit dissipated, and all three methods exhibited comparable performance.[100] This loading-dependent performance occurs consistently and regularly.

4.2. Filler dispersion

Filler dispersion is frequently identified in literature as the primary challenge. Nanofillers possess a large surface area and powerful particle–particle interactions that promote agglomeration.[101,102] Ashraf *et al.* (2018), in a widely referenced modelling work, demonstrated that 2 g of well-dispersed 10 nm nanoparticles generates about 250 m^2 of interfacial area with the polymer matrix; however, aggregation significantly diminishes this effective area and compromises mechanical characteristics.[102] The desired result for clay fillers is exfoliation, which involves the total separation of silicate layers; however, most PS/clay systems approach only intercalation, when polymer chains are introduced between layers without full separation, or exhibit mixed intercalated/flocculated morphologies. Liauw *et al.* (2007) discovered that despite the optimized organophilic alteration of montmorillonite (MMT) by cation exchange, their PS nanocomposites exhibited a mixed intercalated/flocculated morphology without substantial exfoliation.[103] Carastan *et al.* (2010) indicated that block copolymer designs, polystyrene and two styrene-containing block copolymers (styrene–butadiene–styrene and styrene–ethylene/butylene–styrene) attained superior clay dispersion compared to homopolymer PS and that solvent-based mixing surpassed melt processing.[104]

4.3. Industrial bottlenecks

The recent publication addresses the industrial challenge of nanoparticle dispersion, highlighting methods to improve the properties of nanocomposites, including mechanical strength, thermal stability, and conductivity.[105] Mahbubur Rahman *et al.* (2025) address various dispersion methods (*in situ* polymerization, twin screw extrusion, sol–gel processes), while Adrian Moreno *et al.* (2024) identify challenges such as solvent instability and aggregation, highlighting significant gaps. The issue of long-term stability is rarely discussed.[106] Techno-economic analysis is addressed only superficially, emphasizing the commercial viability and life-cycle evaluations of biodegradable polymers as discussed by Swarn Jha *et al.* (2024) and Ravinder Kumar *et al.* (2023).[107,108] Nonetheless, neither analysis PS-based systems directly. The absence of comparative analysis between PS-based composites and other polymers, such as PP, PE, or PVC is emphasized, especially in light of the comprehensive review of PP nanocomposites by Md. Tanvir Hossain *et al.* (2024), which also fails to benchmark against PS. The recognized research gap remains predominantly unaddressed.[109]

4.4. Functional fillers in PS-based composites: a performance comparison

As a carbon-based filler, Moskalyuk *et al.* (2023) showed that the introduction of the layered filler provided the most pronounced rise in the composite rigidity. Compared spherical fullerene, filamentary MWCNTs, and layered graphene platelets in PS developed with the same melt processing method. The stiffness increase was strongest with graphene platelets, followed by MWCNTs, which were intermediate, and finally fullerene, which was the weakest. Below 0.5wt%, reinforcement had no effect and became significant at 5wt%.[110] Composites composed of MWCNT and PS were created by Gündoğan and Karaagac (2025) using injection moulding with a weight percentage of 0.1–0.3 wt%. Of all the loadings tested, the 0.3 wt% MWCNT composite exhibited the greatest tensile strength and elongation as well as the best thermal stability (degradation complete at 539 °C).[111] Carbon nanoparticles/polystyrene (PS)—Inject moulding PS with as little as 0.025 weight percent of carbon nanoparticles increased the material's tensile and impact strengths; however, cracking occurred at higher concentrations.[112] Zhang *et al.* (2024) examined the use of recycled tire lining materials as fillers in PS composites, including ground rubber, carbon black, and textile fibers. The review covered mechanical, flame-retardant, acoustic, and electromagnetic interference (EMI) shielding properties.[113] Li *et al.* (2024) took a broader look at the way a nanofiller geometry includes carbon black (CB), carbon nanotubes (CNTs) and graphene nanoplatelets (GNPs).[114]

Graphene oxide/polystyrene (PS/GO) nanocomposites were studied by Mohammadsalih *et al.* (2023) using peak-force nanomechanical mapping. They found that the PS matrix had a Young's modulus of about 1–2 GPa with well-dispersed GO nanosheets, and the GO content was 1.0 weight percent.[115] The Young's modulus was significantly improved by 122% and 143% at 0.5 and 1.0 wt% GO loading, respectively, when Mohammadsalih *et al.* (2024) used THF for solution casting.[116] In a study conducted by Fatima *et al.* (2024), it was discovered that expanded polystyrene (EPS) with reduced graphene oxide (rGO) had significantly better properties than neat EPS. Specifically, the composite of EPS and rGO resulted in a jump in Young's modulus from 12.4 MPa to 96.3 MPa, and an increase in yield strength from approximately 1 MPa to 46.6 MPa. There was a marked improvement in thermal stability as well. While the addition of polystyrene-*b*-poly(ethylene-ran-butylene)-*b*-polystyrene-grafted maleic anhydride (SEBS-*g*-MA) compatibilizer did improve ductility, it did reduce stiffness slightly.[117]

For PS/silica composites made by melt mixing, Thomas (2024) discovered that the tensile moduli were higher when the silica content was higher. The mechanical properties were improved by adding a half weight percent amino silane coupling agent; the optimal percentage of silica and coupling agent was fifteen weight percent.[118] Improved dispersion, enhanced mechanical properties, and increased thermal stability were reported by Amira *et al.* (2024) for organoclay/PS nanocomposites prepared *via* melt compounding with *N*,*N*,*N*-trimethyl-1-hexadecyl ammonium chloride THDACl-modified

montmorillonite (1–10 wt%).[119] At 5 weight percent clay content, the Young's modulus, impact resistance, and tensile strength were determined to be optimal by Khiati *et al.* (2024) when optimizing PS with Algerian organophilic clay (Maghnite) through *in situ* polymerization.[120] The melt-blended PS/modified sepiolite nanocomposites were created by Ur Rehman *et al.* (2023) using sepiolite clay. The optimal composition resulted in a 48% reduction in burning rate and improved mechanical properties.[121] Organo-montmorillonite (MMT) encapsulation—Akelah *et al.* (2025) achieved exfoliated structures with significantly improved thermal stability by developing a novel miniemulsion polymerization route to encapsulate MMT in PS.[122]

Incorporating metallic NPs with PS composites, PbO/PS—Osman *et al.* (2023) examined bulk and nano-sized PbO (78 nm and 54 nm) in PS, showing that the minimal particle size resulted in improved diffusion and a more robust enhancement of stiffness, with optimal strength achieved at 15 wt%.[123] In a recent review, Kadhim & Hashim (2023) discussed PS doped with metal oxide NPs and their biological and industrial applications.[124]

In general, the results of the current research corroborate previous conclusions: fillers made of graphene or graphene oxide provide the highest mechanical improvements per unit loading, carbon nanotubes provide an optimal combination of mechanical and electrical enhancement, and clays continue to be appealing due to their multifunctional performance, which includes flame retardancy, thermal management, and mechanical properties.

5. Conductive polystyrene composites

An electrically conductive composite is a material that contains sufficient conductive components to ensure consistent and high conductivity, primarily determined by the mobility of electrons. The characteristics of the composite are significantly influenced by the types of fillers used and their interactions with the matrix. Fillers can be categorized into several types, including metal particles like silver, copper, and nickel, high-carbon content fillers, and conductive polymers.[125]

Conductive polymers (CPs) are materials that include polyacetylene (PA), polypyrrole (PPy), polythiophene (PTh), polyfluorenes (PFs), and polyaniline (PANI). Polyacetylene is known for its high conductivity, but it has inferior mechanical properties. Polypyrrole is commonly used in sensors and capacitors, while polythiophene is valued for its electrical conductivity, environmental stability, and versatility in organic electronics. Polyfluorenes are recognized for their luminescent properties, and polyaniline is appreciated for its adjustable conductivity, environmental stability, and ease of synthesis. These conductive polymers can be engineered to enhance conductivity, flexibility, and mechanical characteristics, making them suitable for various applications in electronics, sensors, energy storage, and conversion technologies. This review was described many fabrication methods, and Fig. 7 shows their importance in creating novel conductive textiles.[126]

In detail, conductive polymer-based textiles have been made using CVD, *in situ* polymerization, and electrochemical polymerization, dip coating, spray coating, electrospinning, vacuum filtration, hydrothermal synthesis, and screen-printing. High-performance textiles benefit from CVD's precise polymer layer thickness and homogeneity control. *In situ* and electrochemical polymerisation directly integrate conductive polymers onto fabric, thereby enhancing conductivity and flexibility. Dip and spray coatings apply conductive material consistently and provide patterned designs for specific functions. Electrospinning provides fine fibers for conductivity and surface area, while vacuum filtering adheres conductive layers to porous textiles. Hydrothermal synthesis grows nanostructures to

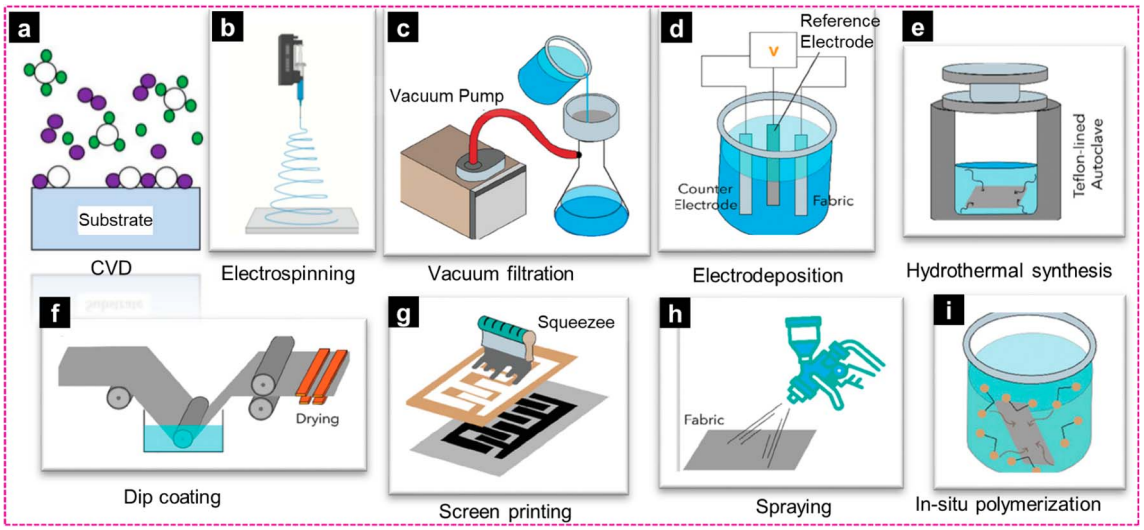

Fig. 7 Schematic fabrication techniques for conductive polymer composites for multifunctional applications. (a) Chemical vapor deposition (CVD), (b) electrospinning, (c) vacuum filtration, (d) electrodeposition, (e) hydrothermal synthesis, (f) dip coating, (g) screen printing, (h) spraying, and (i) *in situ* polymerization. Reproduced from an open access source.[126] [M. A. Shahid *et al.*, 2025], licensed under CC BY.

Table 3 Conductivity of polystyrene and different conductive fillers

Filler type	Electrical conductivity [S cm^{-1}]	References
Silver, gold, iron	10^5	129
Carbon nanotubes	3.8×10^5	128
Graphene	6000	
Graphite	10^4	
Carbon black	$0.1–10^2$	
Silicon, germanium	10^1	129
Doped polyaniline	10^1	
Un-doped polyaniline	10^{-8}	

improve textile electrical properties. In advanced designs, screen-printing allows scalable conductive ink application.

The incorporation of a conductive filler converts most electrically and thermally insulating polymers into semiconductors, thereby improving the electrical and thermal conductivity of polymer composites. Metal fillers, carbon-based fillers, and conductive polymers can enhance the physical properties of polymers, particularly polystyrene (its conductivity 6.7×10^{-14} S cm^{-1}).[127] This is illustrated in Table 3, which compares the electrical conductivity of these composites with that of polystyrene.[128] Moreover, conductive polymers, such as PANI, exhibit electrical conductivity in their emeraldine salt configuration. The conductivity range of PANI varies from $\sigma \leq 10^{-10}$ S cm^{-1} (in the undoped base form) to $\sigma \geq 10$ S cm^{-1} (in the doped salt form).[129]

In the context of conductive nanocomposites based on polystyrene, their potential as advanced adsorbents has been critically reviewed. Table 4 presents an overview of the findings and improvements in conductive nanocomposite ion exchange (IEX) materials for water treatment. Furthermore, the use of conductive polymers, such as PANI, along with low-dimensional carbon materials like carbon nanotubes and graphene and its derivatives, shows promise for enhancing the properties of ion exchange materials at the laboratory scale. This encompasses factors such as the type of conductive filler used, the conditions for composite synthesis, the pollutants removed, the adsorption conditions, the fitting models for isotherms and kinetics, and overall performance efficiency.

5.1. PS polyaniline nanocomposites

Polyaniline (PANI) has garnered significant research interest due to its unique electrical properties and several advantages, including easy synthesis, low cost, and environmental stability. Its reactive NH groups enable the effective adsorption of aquatic pollutants, such as organic dyes, heavy metals, and emerging contaminants. The performance of PANI-based adsorbents can be improved by modifying their shape, pore size, surface charge, and functional groups. These modifications leverage mechanisms like electrostatic interactions and hydrogen bonding.[137] However, the limited mechanical properties and solubility of PANI can be enhanced through various synthesis techniques, including the development of composites with materials such as silica, carbon nanotubes, and metal–organic frameworks.[129,138]

Polyaniline-based composites, created by mixing polyaniline with one or more similar or different materials, have demonstrated effectiveness as adsorbents capable of extracting and detoxifying various contaminants, including heavy metals.[139] Additionally, PANI serves as an effective platform for heterogenizing catalysts, and copolymerization can enhance the properties of the resulting materials. Ion exchange with heavy metals has also been reported in PANI-PS-based adsorbents.[140] To remove arsenic(III) and (V), polyaniline (PANI) is coated onto polystyrene nanoparticles. The presence of aniline's amine group allows it to effectively absorb anions like arsenic. The synthesized polyaniline, which contains small dopants such as Cl^-, ClO_4^-, and SO_4^{2-}, demonstrates an anion-exchanger behavior due to the mobility of ions within the polymer matrix. In contrast, cation exchange occurs with larger dopants, such as polystyrene sulfonate, because of their immobility within the polymer matrix.[132] The PANI/polystyrene composite has been studied for its ability to adsorb Hg(II), Pb(II), and Cr(VI) ions from solutions. Researchers have explored effective methods to incorporate PANI chains into pristine PS mats without compromising their porosity or mechanical flexibility. The resulting composites feature nanostructured PANI chains dispersed throughout the PS mat, enhancing their electrical and surface-wetting properties. These polymers contain numerous amine and imine functional groups, which enable strong interactions with metal ions that have a high affinity for nitrogen.[131,133] To identify trace amounts of atrazine (ATZ) in water, we polymerized PANI into biochar (BC) particles using polystyrene sulfonate (PSS). This process created a conductive and electrochemically active layer by synthesizing PANI and then applying a composite of BC nanoparticles modified with PSS onto a screen-printed electrode. Bovine serum albumin (BSA) is used to block non-specific binding sites, while the anti-ATZ antibody is covalently attached to the PANI. Sugarcane biochar is an affordable and highly conductive material with a large surface area, which makes it an excellent choice for linking PANI and PSS. This methodology leads to the development of electrochemical immunosensors for detecting ATZ.[141]

The use of polystyrene-based sorbents has been improved for the extraction of psychoactive drugs from biofluids by incorporating polyaniline and zirconium dioxide (ZrO_2) particles. Specific triazines were extracted from water samples using polyaniline (PANI)-based fibers *via* flow injections. Although polyaniline is not commonly used for extracting drugs from biological samples, it is primarily employed for removing organic dyes and heavy metals from water using sorbent materials. The specific surface area of untreated polystyrene fibers increases when they are doped with zirconium(IV) oxide particles or polyaniline, enhancing their sorption capabilities. This modified material can effectively remove certain compounds from urine and plasma.[142] The nanofibrous polyaniline–polystyrene–sulfonate sensors effectively detect ammonium ions (NH_4^+) and urea in a urine model that contains chemical interferences. The reversible doping and de-doping mechanism enables PANI to sense non-charged ammonia

Table 4 Conductive PS composites

Conductive filler	Synthesis conditions	Pollutant	Adsorption conditions	Performance efficiency	References
(I) PS PANI					
PANI	Electrospinning produced PS fiber mats, and chemical oxidation produced conductive (PANI) polymer. A PANI added to the PS solution and agitated for 24 h to synthesize conductive (PS/PANI) fibers	Oil water separation	Dispersed crude oil (mixture of 10 mL crude oil with 100 mL water) Time 120 min	Oil-Q_{Max} 71.5 g g^{-1} Reusability: 3 cycles	130
PANI	A polymeric composite mat presenting a hierarchical structure produced by the *in situ* chemical polymerization of aniline on electrospun PS fibers performed at RT for 24 h	Pb(II), Cu(II), Hg(II), Cd(II), and Cr(VI)	pH 4 Temp. 25 °C	Qe Pb(II) 312 mg g^{-1} Cu(II) 171 Hg(II) 148 Cd(II) 124 Cr(VI) 58	131
PANI	Preparation of PS core latex by microemulsion polymerization. The nanocomposite prepared by coated (PANI) onto (PS) NPs in presence of different stabilizer as hydroxyl propyl cellulose (HPC), and sodium dodecyl benzene sulfonate (DBSNa), for 4 h at RT	Arsenic As(III), As(V)	Dose 10 g L^{-1} Ci 1 mg pH 8 Time 30 min	As(III)-Qe 56 mg g^{-1} As(V)-Qe 52 mg g^{-1} Langmuir and Freundlich	132
PANI	After a microemulsion polymerization of PS, an aniline monomer was added to solution containing ps, ammonium peroxy disulfate (APS), poly (vinyl pyrrolidone) (PVP), for 4 h in RT	Cr(VI)	Dose 15 g per L pH 4 Time 30 min	Cr-Q_{Max} 19 mg g^{-1} Reusability: 3 cycles Temkin, Pseudo-second-order	133
(II) PS carbon NPs					
Activated carbon (AC)	AC prepared from biomass of pomegranate peels waste, then AC-PS fibers fabricate *via* electrospinning technique, a spinning solution prepared by mixing PS, AC, and solvent at 50 °C for 2 h	Crystal violet (CV) dye	Dose 1 g L^{-1} Ci 200 mg per L pH 10 Temp. 25 °C Time 24 h	CV-Qe 403 mg g^{-1} Reusability: 10 cycles Langmuir Pseudo-second-order	134
Carbon nanoparticle (CNPs)	Polyacrylonitrile/polystyrene/CNP-based foams designed, fabricated, the final mixture refluxed for 2 h at 120 °C	Pb(II)	Ci 100 mg per L pH 3	Pb(II)-Qe_{Max} 166 mg g^{-1}	135
Graphene oxide (GO)	Core–shell PS/GO prepared by pickering emulsion method. Styrene added dropwise to graphene dispersion solution in presence of Azodiisobutyronitrile (AIBN) then stirred and cross-linked at 75 °C for 20 h	Rhodamine B (RhB) Methylene blue (MB)	Ci 300 mg L^{-1} Dose 0.1 g pH 7 T 55 C time 2 h	RhB-Q_{Max} 49.70 mg g^{-1} MB-Qe_{Max} 59.07 mg g^{-1} Reusability: 5 cycles Langmuir Pseudo-second-order	136

(NH_4^+) by utilizing the lone pair of electrons on the nitrogen atom for interaction. Additionally, by incorporating enzymes such as arginase and creatinase, which are responsible for detecting L-arginine and creatinine, respectively, the NH_4^+ sensitive nano-PANI:PSS interface can be utilized to construct biosensor systems.[143] A water–dispersible complex of polyaniline and sulfonated polysulfone was created through spray coating and has been found to be highly sensitive to ammonia in the air. To detect ammonia vapor within a concentration range of 25 to 52 ppm corresponding to the organoleptic detection limit of ammonia and the maximum allowable concentration in the workplace the PANI-SPS complex films were tested as sensitive layers in optical sensors.[144] The adsorption of oil contaminants can be effectively achieved using a combination of hydrophobic polystyrene (PS) fibers and conductive PANI nanoparticles. These porous and hydrophobic PS/PANI fibers exhibit a high capacity for adsorbing various types of oil. PANI, a conductive polymer, enhances the properties of electrospun fibers. Compared to PS fibers, the conductive fibers offer improved microstructure and performance. As selective adsorbents, the conductive and hydrophobic PS/PANI fibers are capable of absorbing several oils.[130]

A composite membrane that is resistant to acids and has an enhanced ability to recover flux has been developed for use in treating acid wastewater. This was achieved by *in situ* coating a polyvinylidene fluoride (PVDF) membrane with protonated polystyrene sulfonic acid (PSSA)-doped polyaniline. The membrane demonstrated an impressive flux recovery rate of 95%, showcasing its exceptional anti-fouling properties. By applying specific coating components, it became feasible to create membranes that resist acid, which represents a promising and effective approach. The choice of coating components is crucial for achieving acid resistance. Furthermore, improved resistance to corrosive environments can be attained by doping PANI, a polymer composed of benzene and quinone rings, with various protonic acids.[145] Researchers developed environmentally friendly PS/PANI anticorrosion coatings using PS foams, achieving a protective efficacy of 99.99%. The coatings were produced through a non-toxic PANI seed-polymerization method. They exhibit excellent adhesion, low shrinkage, ductility, and insulation properties.[146]

Considering the wide range of conductivity required in the electronics industry, these mixtures could be used in various electronic applications, including packaging, textiles, and electronic devices. One notable use for PANI/PSSA composites is as a coating for textiles that serve as flexible semiconductors. There are two methods for coating conducting textiles with PANI-polystyrene sulfonic acid (PSSA): the aqueous procedure and the emulsion route.[147] Green *in situ* chemical polymerization was used to produce PS/PANI nanocomposites. The electrical conductivities of the composites ranged from 10^{-3} to 10^{-4} S cm^{-1}, indicating that PANI enhances electrical properties, as evidenced by the high decomposition temperatures of PS. These composites have potential applications in antistatic and charge dissipation technologies.[148] The solution-cast PANI/PS-MWCNT composite demonstrated excellent electromagnetic shielding conductivity. There was an improvement in conductivity by approximately three orders of magnitude, and the percolation threshold was very low. The electrical conductivity of the PANI/PS-MWCNT nanocomposite film was significantly enhanced by the incorporation of MWCNTs. At room temperature, the electrical conductivity of the PANI/PS nanocomposites is measured at 3.73×10^{-6} S cm^{-1}, whereas for PANI/PS-MWCNT, it rises to 5.72×10^{-3} S cm^{-1}. Additionally, the inclusion of MWCNTs changes the PANI/PS film's conductivity type from p-type to n-type.[149] There is significant potential in the field of intelligent thermal control for satellites that utilizes infrared electrochromic devices made from polyaniline (PANI) to manage infrared radiation. A PANI film exhibiting a compact micromorphology and exceptional infrared electrochromic properties was developed by incorporating a small amount of PSS into the electrodeposition solution.[150] The PANI blends were developed by combining various types of polymers, including sodium alginate (SA), PVC, PS, and PVA. Among these blends, the PANI-PVA combination stands out with a conductivity of approximately 1.22×10^{-4} S cm^{-1}, making it the most promising option for a variety of electrical applications. The PANI-PS blend follows closely behind, exhibiting a conductivity value of 9.27×10^{-5} S cm^{-1}.[151] A core–shell nanocomposite of conductive polyaniline-*g*-polystyrene/Fe_3O_4 was synthesized. This process involved functionalizing styrene with amine groups using atom transfer radical polymerization, which was then combined with aniline through surface oxidative graft copolymerization. The resulting conductive polymer/Fe_3O_4 nanocomposites exhibit high electrical conductivity (1.25 S cm^{-1}) and thermal stability, making them beneficial for supercapacitors, electronic devices, and medical applications.[152]

5.2. PS carbon nanocomposites

Fillers containing over 90% carbon are primarily used for their excellent electrical conductivity. High-carbon fillers include carbon black (CB), graphite, expanded graphite, carbon nanotubes (CNTs), graphene, and reduced graphene oxide (rGO).[125]

Research has been conducted on composites made from polystyrene nanoparticles and MWCNTs to explore their potential applications in electromagnetic interference (EMI) shielding and microwave attenuation. Among the nanoparticle morphologies studied, graphene oxide (GO) and spherical iron oxide (Fe_3O_4) demonstrate distinct characteristics. These nanoparticles were incorporated into a composite of recycled polystyrene and MWCNTs, referred to as the PS-MWCNT composite, using a process known as nanoinfiltration.[153] Yang *et al.* (2016) reported a maximum conductivity of 1.1×10^{-6} S m^{-1} when constructing a conductive polymer nanocomposite using multi-walled carbon nanotubes (MWCNTs) in a foam structure, along with a polyelectrolyte called PEDOT:PSS. This approach reduced resistance at the inter-tube junctions and resulted in increased conductivity.[154] Ahmed *et al.* (2016) found that chemically linked interpenetrating networks enhanced the electrical conductivity of composites made from polyurethane, polystyrene with aminofunctional groups, and multiwall carbon nanotubes. These composites exhibited excellent shape memory properties and

achieved an electrical conductivity of 1.08 S cm^{-1}. The incorporation of nitro- and amino-functional groups into polystyrene led to the formation of these matrices. This nanocomposite, consisting of PS and PU, demonstrates promising shape recovery capabilities.[155] Increasing the amount of carbon nanotubes (CNTs) in polystyrene enhances its direct current electrical conductivity. Additionally, as both the frequency of the applied electrical field and the weight percentage of CNTs in the composites increase, the alternating current (AC) electrical conductivity also rises. This improvement is accompanied by increases in the absorption and extinction coefficients, the refractive index, and both the real and imaginary components of the dielectric constants.[156]

Polystyrene/graphene nanocomposites have been investigated for potential anticorrosion and electromagnetic interference shielding applications due to the enhanced mechanical and thermal properties that can be achieved by incorporating graphene as a nano filler.[157] Graphene enhances the mechanical and thermal properties of sulfonated polystyrene (SPS). SPS particles adhere to graphene surfaces due to the interactions between the functional groups of GO and the $-SO_3H$ groups in SPS. These SPS particles contribute to the formation and stabilization of single-layer graphene sheets, resulting in a mechanically robust and ion-conducting SPS resin. Additionally, this resin can withstand challenging conditions found in wastewater treatment, making it a stable and effective raw material.[158] Nanocomposites made from vinyl polymer and graphene have demonstrated potential as effective corrosion preventive materials. Using *in situ* miniemulsion polymerization, researchers developed nanocomposites that exhibited improved corrosion resistance, specifically PS combined with modified GO. These nanocomposites not only showed enhanced mechanical properties but also improved gas barrier qualities and thermal stability. According to a study by Yu *et al.* (2014), there was a notable reduction in nitrogen permeability, with decreases of 25% and 60%.[159] The electrical conductivity of PS composites was improved by functionalizing the surface and reducing GO with octadecylamine (ODA), eliminating the need for additional reducing agents. The hydrophilic GO transformed into a more hydrophobic form due to the extended octadecyl chain. Furthermore, the process of compression molding contributed to a slight enhancement in conductivity.[160]

Microfibers made from activated carbon (AC) and polystyrene (PSF) were created using an electrospinning process. The AC-PSF composite offers a promising solution as an adsorbent for removing cationic dyes from contaminated water due to its simple design, high reusability, and ease of handling. By integrating activated carbon into the polystyrene fibers, we were able to enhance and roughen the surface structure. With a point of zero charge (pHpzc) of 3.5, the AC-PSF composite benefits from an increase in adsorption sites on the fiber surface, attributed to the presence of activated carbon.[134] Microspheres made from a composite material consisting of polystyrene and graphene oxide can effectively capture dye contaminants. These microspheres, featuring a PS-GO layered composite, were produced using the Pickering emulsion technique, with styrene acting as the soft film and GO serving as the shell. The adsorption of rhodamine B (RhB) and methylene blue (MB) dyes in a synthetic solution was examined using the PS-GO composite. Due to its various hydroxyl, carboxyl, and epoxy groups, GO exhibits remarkable mechanical, electrical, and thermal properties, in addition to being amphiphilic and easily dispersible. The presence of oxygen-containing functional groups generates several interlayer negative charges, which enables the removal of certain cationic pollutants through electrostatic attraction.[136]

A blend of polyacrylonitrile and polystyrene (PAN/PS) was synthesized using acid-functional carbon nanoparticles, resulting in a PAN/PS/CNP nanocomposite foam. This new foam demonstrated a 30% greater water absorption capacity compared to the pure foam. Additionally, it effectively removed hazardous Pb^{2+} ions with an efficiency of 99%, significantly higher than the 45% efficiency of the PAN/PS foam. The development of this nano cellular foam for metal ion removal involved careful design of the structural mix and the incorporation of functional nano fillers. These foams exhibit excellent performance and are also heat and flame retardant.[135] Toluene is an organic contaminant, and the effectiveness of removing it using PS-MWCNTs-Fe nanocomposites improved when magnetite and polystyrene were combined. Nanoparticles exhibit remarkable qualities such as a higher sorption rate, super-hydrophobicity, and super-oleophilicity. These characteristics form the basis for the various applications of nanotechnology.[77] Furthermore, a nanocomposite of MWCNTs and polystyrene–divinylbenzene (PS-DVB) resin, produced through suspension polymerization, enhanced the mechanical properties and ion exchange capacity in saltwater, resulting in an increase of cation exchange from 225 to 446.6 meq/100 g of CNTs.[161]

5.3. Conductive fundamental mechanisms

Two related factors influence the electrical performance of conductive composites made from polystyrene: the interfacial interactions at the polymer–filler interface and the conduction mechanisms among the filler particles, which create particle networks. Recent modeling efforts have significantly clarified these relationships. Below the percolation threshold, the primary mechanism for charge transport is electron tunneling between neighboring conductive fillers that are separated by thin layers of polymer. Above the percolation threshold, however, ohmic conduction through direct contacts between fillers becomes the dominant mechanism.[26,27] Tunnelling conductance diminishes exponentially with inter-particle distance, and recent models by Zare *et al.* (2025) indicate that tunnelling distances exceeding approximately 5–6 nm result in a composite insulator, whereas distances of 1–2 nm optimise conductivity.[29] Payandehpeyman and Mazaheri (2022) presented a comprehensive micro-mechanical model indicating that the aspect ratio of fillers is significant in determining the percolation transition: fillers with extreme aspect ratios (below 10^{-2} or above 10^{2}) enable a metallic-like conduction, whereas intermediate aspect ratios tend towards insulating characteristics.[30]

The interactions at the interfaces between the conductive fillers and the polymer matrix are equally important. The effective concentration of fillers, overall bulk conductivity, and the connectivity of the network are all influenced by the interphase, which is a thin layer of polymer surrounding each filler particle and possessing the necessary properties. Recent studies indicate that a thicker interphase reduces the percolation threshold and improves conductivity by increasing the effective volume of each filler particle, whereas insufficient interfacial conduction (below approximately 200 S m^{-1} for graphene systems) can make the composite insulative independent of filler concentration.[28] Apátiga *et al.* (2021) employed Monte Carlo simulations to demonstrate that non-covalent interactions, specifically π–π stacking between aromatic polymers such as polystyrene and graphene, enhance the electron mean-free path and facilitate the percolation transition, leading to PS more advantageous as a matrix for graphene-based composites in comparison to non-aromatic polymers.[162] Research conducted by Han *et al.* (2022) established that enhanced physical interfacial interactions between the matrix and filler facilitate the development of thermally and electrically conductive filler networks, and that hybrid filler systems, which integrate laminar and spherical nanoparticles, can further improve network connectivity.[163]

Three fundamental charge transport mechanisms exist in PS-based conductive composites, dependent on filler loading and temperature: fluctuation-induced tunneling (FIT), variable-range hopping (VRH), and simple ohmic conduction. FIT, the most significant mechanism, involves thermally activated voltage fluctuations leading to tunneling conductivity as first defined in the seminal work by Sheng *et al.* (1978) in carbon-PVC composites and further confirmed in PS/CNT composites by Kažukauskas *et al.* (2008).[31–33] D. Petras *et al.* (2013) noted that the PS matrix alters conduction in CNT networks, decreasing temperature dependence.[164] VRH dominates at low temperatures where carriers hop between localized states; Francis *et al.* (2019) identified insulating and metal-to-insulator transition regimes in PS/MWCNT and PS/RGO composites, noting a crossover with FIT around 90 K.[165] Simple ohmic conduction occurs above the percolation threshold when a continuous conducting pathway forms, with Ambrosetti *et al.* (2010) indicating tunneling behavior dominates when the ratio of particle size to tunneling length is below 5.[166] Mergen *et al.* (2020) found varying percolation thresholds in PS/GNP and PS/MWCNT composites, supporting three-dimensional filler network behavior.[167]

6. Superconductive PS composites

6.1. The difference between conductive and superconductive materials

Characteristics such as electrical resistance, critical temperature, magnetic field response, critical current density, and energy gap, generally define the difference between conductive and superconductive materials. The main characteristics are described as follows:

- Electrical Resistivity | normal conductors, such as copper, have an electrical resistivity of approximately 1.7×10^{-8} Ω m at ambient temperature. This value decreases to around 10^{-10} Ω m at cryogenic temperatures, but it never completely disappears because to lattice imperfections, so hence, there is always some residual resistance.[168] In contrast, superconductors exhibit a DC resistivity of zero below their critical temperature (which has been experimentally shown to be less than 10^{-25} Ω m),[13]

- Critical temperature (T_c) | below this level, superconductors are only effective. Type I conventional superconductors, such as aluminium (1.2 K), lead (7.2 K), and niobium (9.3 K), have extremely low T_c values. Type II superconductors, such as NbTi (with a T_c of around 9.8 K) and Nb_3Sn (with a T_c of about 18 K), are the mechanically strong ones.[169] Bi-2223 at around 110 K, YBCO at around 92 K, and Bi-2212 at around 85 K are all examples of high-temperature superconductors that significantly raised this.[14,15] The resistivity of ordinary conductors just drops steadily as they cool; there is no such transition.

- Magnetic field response | is a phenomenon known as the Meissner effect, in which superconductors show the internal magnetic flux completely expelled. This results in perfect diamagnetism with a magnetic susceptibility of $\chi = -1$.[16] A diamagnetic response ($\chi \approx -10^{-5}$ for copper) is the weakest observed in normal conductors. At low temperatures, YBCO films may exceed 100 T, whereas Nb_3Sn has an upper critical field of roughly 24–28 T and Type II superconductors can function under even higher fields (*e.g.*, lead at around 0.08 T). Superconductivity is lost above a critical magnetic field.

- Critical current density (J_c) | the highest current that can be carried by a superconductor without any resistance. What a major achievement for technological superconductors. At 77 K with no applied field, YBCO thin films may achieve 20 000 A mm^{-2},[17] whereas NbTi wires can transport around 3000 A mm^{-2} at 4.2 K and 5 T. Typical copper wire, on the other hand, has a heating limit of 5–10 A mm^{-2} rather than a basic limit that is around 1000 times lower.

- Energy gap | the binding energy of Cooper pairs is denoted by the BCS energy gap, which exists in superconductors.[13] The gap measures around 20–40 meV for YBCO and 3 meV for niobium. In typical conductors, conduction electrons do not encounter a gap due to a constant density of states at the Fermi level.

6.2. Superconductivity measurements

The way materials respond to magnetic fields and their ability to conduct electric current determines whether they are conductive or superconductive. Superconducting materials exhibit zero electrical resistance below a specific temperature, while materials with low electrical resistance need to be cooled below this critical temperature to achieve superconductivity. Key characteristics of superconductivity include the Meissner effect, which expels magnetic fields, and the complete absence of electrical resistance. Researchers use both theoretical models and experimental methods to measure and predict superconductivity.

Six essential parameters are crucial for measuring superconductivity: electrical resistivity (ρ), magnetic susceptibility

(χ), critical temperature (T_c), critical magnetic field (H_c), critical current density (J_c), and heat capacity. Electrical resistivity (ρ) measures a material's electrical resistance per unit length and cross-sectional area, while magnetic susceptibility (χ) evaluates how much a material becomes magnetized in an external magnetic field. The critical temperature (T_c) indicates the temperature below which a material exhibits superconductivity, with higher T_c values being more desirable for practical applications.

The critical magnetic field (H_c) denotes the maximum magnetic field strength a superconductor can tolerate before reverting to a normal state, which influences its applications in magnets and electronic devices. Critical current density (J_c) represents the maximum current per unit cross-sectional area that a superconductor can carry without losing its superconducting properties, impacting its use in power transmission, magnetic systems, and various devices. Heat capacity measures the amount of heat needed to change the temperature of a given amount of material by 1 K, and it significantly increases at T_c due to the formation of the superconducting energy gap.[170,171]

6.3. Predicting superconductivity

Predicting superconductivity is a complex task because of the intricate quantum interactions involved. Current methods include empirical and phenomenological models, Bardeen–Cooper–Schrieffer (BCS) theory, density functional theory (DFT) combined with Eliashberg theory, machine learning (ML) approaches, and high-throughput screening. Several factors influence superconductivity, such as crystal structure, electron density, lattice vibrations, doping concentration, and pressure.[172–174]

Accurate predictions of superconducting transition temperatures (T_c) for new materials can be achieved using various theoretical and machine learning approaches. However, there is no single method that stands out as the best. The evidence presented evaluates several methodologies along with their respective performance metrics. Machine learning models give the most accurate quantitative results. For example, in 2023, Jingzi Zhang *et al.* developed an integrated algorithm to achieve $R^2 = 95.9\%$; in 2026, P. A. H. Nawoda reported $R^2 = 93\%$ using light gradient boosting; and in 2025, Siwoo Lee applied ridge regression to achieve ± 5 K prediction errors.[175–177]

Examination of the critical temperature of superconductors by means of numerical methods predicated on electron–phonon interactions makes use of a particular equation designed to estimate T_c.[178] Using the Eliashberg spectral function, there has been some theoretical work to determine the critical temperature in relation to pressure. Take the hypothetical discovery of a new material as an example of how to measure and predict T_c. The following steps are involved in determining T_c: measuring it with resistivity and magnetic susceptibility; computing its structure using X-ray diffraction (XRD) and DFT; and lastly, predicting its value using phonon calculations based on Eliashberg theory and ML models developed on known superconductor data. The BCS hypothesis is the one that has been found to accurately explain superconductivity's characteristics. Cooper pairs, which are essentially electron pairings, are the primary process that transforms a regular conductor into a superconductor. Another common approach is to combine lattice structure search with DFT. To find the solution to the Eliashberg gap equation. Considering the Allen–Dynes formula, through providing a clear description of the spectral function's significance in estimating superconducting features.

6.4. Superconductive polymeric nanocomposites

Superconductive polymeric nanocomposites are hybrid materials that blend organic polymer matrices with superconducting nanoparticles or fillers.[14,15] A method for creating processable, flexible superconducting composites by inserting high-temperature superconducting ceramic particles (YBCO, BSCCO) into polymer matrices, including polyethylene, poly(-methyl methacrylate) (PMMA), and polystyrene. To address the challenges of processing bulk superconductors into fibers, coatings, or flexible films, areas where they are either too heavy or too brittle to create processable materials that are both lightweight and flexible, while acquiring superconductive properties from nanoparticles. This will improve their mechanical strength, film-forming capability, and chemical stability. The composition, dispersion, and connectedness of the fillers are crucial to the superconductivity. For fabrication, processes like *in situ* polymerization or solution casting, nanoparticles are mixed with a PS solution and then cast into films. Mixed solid PS and filler at high temperatures is called melt blending; this method is less often used because of thermal limitations. Nanofiber mats having superconducting properties were created *via* electrospinning. Flexible superconducting wires, low-temperature sensors, quantum electronic circuits, cryogenic electromagnetic interference shielding, magnetic shielding films, and experimental/conceptual applications.

6.5. Examples in the superconducting PS nanocomposites

The electrical impedance and diamagnetic response methods are the most common ways to evaluate the superconductivity in polystyrene nanocomposites. The ability to conduct electricity is a result of the polymer chains being intercalated into the grain structures of ceramics. Several important studies use different measuring techniques, according to the available evidence. R. Abraham *et al.* (2010) investigated the dielectric mixing rules for composites containing superconductor ceramic particles (YBCO) distributed in a (PS) matrix with (0–3) connectivity in this study. The composites were prepared using the melt mixing approach, which eliminated the need for solvents during the ceramic filler's mixing process. Here we show the findings of phase angle *vs.* temperature and impedance *versus* frequency (100 Hz–13 MHz) for volume percentages of superconductor (0–40%). One of the most popular methods for estimating the bulk dielectric characteristics of non-uniform materials is the Clausius–Mossotti equation, which the system follows. After passing over YBCO's superconducting transition temperature,

the composites' impedance and phase angle did not undergo any noticeable abrupt changes.[18]

Y. Vidadi *et al.* (1994) assessed diamagnetic responses at 50 kHz relative to the high-T_c superconductor (HTSC) concentration in PS-$YBa_2Cu_3O_{7-\delta}$ composites (ranging from 0 to 100 vol% in 5% increments) and temperature (T = 77–300 K), finding a critical percolation (C) threshold between 0.20 and 0.30, where electrical resistance decreased from 10^{14} to 10^4 Ω cm. The enhancement of the diamagnetic response in composites with elevated C is attributable to the creation and mixing of a complex, superconductive labyrinth composed of $YBa_2Cu_3O_{7-\delta}$ grains.[19]

Tonoyan studies (2009, and 2013) provided the foundation for a mechanism for superconducting characteristics by explaining how ceramic interstitial layers may be used to intercalate macromolecule fragments. The SC properties of the nanocomposites made of $Y_1Ba_2Cu_3O_{7-x}$ ceramic (t press. = 130 °C, τ press. = 4 min) using PS as an illustrative binder, the compositional content in the binder (10, 15, 20%), and T_c values ranging from 92 to 93 K. This process alters the morphological structure of SC nanocomposites. On the other hand, these sources omit information on quantitative predictive models.[14,15]

Through improved field effect and charge transport, liquid crystals (LCs) with graphene oxide (GO)-doped dimethyl sulphate (DMS)/poly(3,4-ethylenedioxythiophene):polystyrene sulfonate (PEDOT:PSS) superconductive alignment layers achieve competitive optoelectrical switching properties and non-residual direct current performance. The DMS/PEDOT:PSS solution with a weight ratio of 1 : 25 was doped with GO at 0.2, 0.5, or 1.0 mg g^{-1}; the composite solution was agitated continuously for 6 hours at 16–18 °C. After spin-coating substrates with GO/DMS/PEDOT:PSS composite solution, a nylon roller rubs them. Conductivity increased significantly with GO weight concentration, rising from 132 S cm^{-1} in the pristine thin layer to 210.29 S cm^{-1} at 1.0 mg per g GO.[20]

The critical temperature (T_c) of a variety of sintered and non-sintered polymeric superconducting systems has been found by combining two extrinsic conducting polymer systems, PVDF/PS/carbon black and PVDF/PS/copper, with the superconducting ceramic YBaCuO. Susceptibility measurements as a function of temperature have also been used to study the diamagnetic properties of these systems. Experiments show that unsintered systems exhibit metallic-like conductivities in samples with the highest carbon black content and that copper-based composites are insulating. Electrical superconductivity is indicated by the absence of a sharp rise in conductivity with increasing temperature in these systems. Whenever the critical temperature range is brought closer to 100 K, the presence of a superconducting transition is shown by magnetic susceptibility measurements. The mechanical characteristics and shape of the samples were maintained during sintering. The electrical conductivity study verified that the superconductivity in YBaCuO, which had been shown by X-ray evidence, was eliminated during sintering due to polymer combustion.[21]

Superconductivity in graphite-sulphur composites is significantly influenced by electron–electron correlation, displaying distinct characteristics within certain domains. According to Ionov (2021), r-GO is a promising material for developing organic–inorganic composites with notable electrical and magnetic properties. The composite magnetization loops exhibit type-II superconductivity at room temperature, attributed to the adhesion of r-GO flakes to a polymeric matrix. Additionally, another enhanced article by the same authors provides alternative interpretations of the ferromagnetic hysteresis loop observed in UV-rGO. UV-reduction techniques create submicron voids within r-GO flakes, leading to edge defects that may induce magnetic order in graphite samples.[22,23]

In the polymer/carbon nanotube composite, carbon nanotubes act as exceptional fillers for the polymers. The phenomenon of electromagnetic interference shielding in polystyrene/carbon nanotube composites results from properties that can rival those of traditional shielding materials.[24] Recent research has demonstrated that superconducting single-walled carbon nanotubes (SWCNTs) can reduce the electrical resistance of composite materials. Studies have investigated how various factors, such as surface functionalization of SWCNTs with methacrylate groups, copolymerization with styrene, precipitation conditions, disintegration, and polymer composite coatings, influence the electrical conductivity of one-dimensional carbon fillers. Additionally, covalent bonding with the polymer matrix can induce mechanical stress, which may affect the electronic structure of the carbon inclusions.[25]

6.6. Superconductive fundamental mechanisms

The development of superconductivity in PS composites is a different phenomenon, as it does not originate from the polymer but rather from the incorporation of ceramic superconductor particles (YBCO) into the PS matrix. While the polymer acts as a deformable and processable host, the ceramic filler is completely accountable for the superconducting properties. The diamagnetic response, a characteristic of superconductivity, follows percolation behaviour with a critical YBCO volume fraction between 20–30%, according to research by Vidadi *et al.* (1994) on PS/YBCO composites.[19] Critically, the polymer matrix does not contribute in the superconducting transition. Based on their measurements of YBCO/PS composite impedance, Abraham *et al.* (2010) concluded that the composite acts as a dielectric, with the YBCO adding polarisability but no macroscopic superconductivity in the bulk, and that there is no noticeable change in phase angle at the filler's superconducting transition temperature.[18] According to Río & Acosta (1996), a study on PVDF/PS/carbon black systems that were loaded with YBCO revealed that although there was a superconducting transition near 100 K as measured by magnetic susceptibility, there was no sudden increase in electrical conductivity. This suggests that isolated superconducting grains can show diamagnetism without creating a continuous superconducting path. Very high ceramic loading (above percolation) or post-processing, such as sintering, is required to achieve zero resistivity in these composites; however, sintering can degrade the superconducting orthorhombic phase through polymer combustion, though.[21]

Superconductive section concludes, with a three-part focus on the review's core topic : polymeric nanocomposites, with a particular emphasis on polystyrene, and superconducting measurements and predictions. Superconductivity measurements indicate that superconductors exhibit negligible resistance below a certain temperature (T_c). Electrical resistivity, magnetic susceptibility, critical current density, critical magnetic field, and heat capacity are important criteria for determining superconductivity. As a distinguishing feature, the Meissner effect is emphasized. Researchers make predictions about superconductivity using tools such as density functional theory, BCS theory, machine learning, and empirical models. Improvements in the accuracy of predictions, especially those made using machine learning, are highlighted. Superconductive polymeric nanocomposites combine organic polymers and superconducting nanoparticles, enhancing mechanical characteristics while preserving superconductivity. Methods for evaluating electrical impedance and diamagnetic responses in superconducting polystyrene nanocomposites are illustrated. Research shows that processing and material composition affect superconductivity, and that the field has its own set of difficulties, such as making accurate quantitative predictions of superconductivity.

7. The correlation between water treatment and conductive/superconductive applications

The utilization of polystyrene (PS) nanocomposites in water treatment and conductive/superconductive applications is in harmony. Dispersion, interface engineering, and hierarchical structuring are materials science strategies that align with the opportunities for multifunctional devices, which include electrically-assisted filtration, photocatalysis, and magnetically recoverable adsorbents. Using layered/core–shell architectures, hybrid fillers, and suspension techniques, we may overcome the major tensions between hydrophilic, high-surface-area designs for water treatment and dense, percolated filler networks needed for high electrical conductivity. While some opportunities for multifunctional devices do exist in the literature, a broad range of research has concentrated on single functions rather than integrated systems.

Electrically-assisted filtration/adsorption, numerous studies on electrically-assisted filtration/adsorption, and the electrical enrichment of adsorption processes. Mahdi *et al.* (2020) demonstrated that electro-assisted adsorption enhanced heavy metal removal by 21–94% relative to unmodified adsorbents.[179] Xiong *et al.* (2020) demonstrated the efficacy of electrosorption technology for the removal of nanoplastics, indicating its potential as a tertiary treatment method in wastewater treatment facilities.[180] Ding *et al.* (2024) developed conductive adsorbents that facilitate electrically controlled desorption with an efficiency of 94.1% and bias-dependent sequential release capabilities for mixture separation.[181] Photocatalytic Integration, S. Wanjale *et al.*, 2016, developed PS/TiO_2 composite nanofiber membranes, wherein TiO_2 nanoparticles provide associated photocatalytic properties, increase hydrophilicity, and accomplish a considerable Cu^{2+} adsorption capacity of 522 mg g^{-1}.[182] Xiong *et al.* (2020) utilised UV radiation to model ageing processes, exhibiting light-responsive behaviour in nanoplastic systems.[180] Electrochemically Reversible Systems, Ren *et al.*, 2018 developed electrochemically regenerable polymeric adsorbents utilising surfactant-doped conducting polymers, attaining a pollutant capacity exceeding 570 mg g^{-1} of polymer through electrochemical control of hydrophobicity for multiple adsorption/desorption cycles.[183]

Limitations, the existing sources lack evidence for magnetically recoverable adsorbents or fully integrated multifunctional devices that include all three functionalities. Numerous studies illustrate singular functionalities or dual-function systems, highlighting prospects for the creation of more integrated multifunctional platforms.

8. Concluding remarks

This review highlights the significant advancements in the development of conductive and superconductive polystyrene-based nanocomposites. By incorporating various fillers, such as metal and metal-oxide nanoparticles, clays, silica, carbon nanostructures, and polyaniline, these polystyrene-based composites have showcased multifunctional capabilities in several areas, including adsorption, catalysis, energy storage, sensing, electronic devices, and environmental remediation. Hybrid designs that merge the large surface area of nanoparticles with the chemical adaptability of polystyrene resins present numerous opportunities for addressing environmental and electronic challenges. Table 5 summarizes the information and provides an analysis of the common findings discussed by the authors.

To achieve characteristics like diamagnetism (the Meissner effect) and zero resistance, superconductive PS composites mix polymer matrices with superconducting nanoparticles (such as YBCO). Measurements like energy gaps, critical current density, and critical temperature are used to evaluate superconductivity, with the help of prediction models. Achieving a high enough volume fraction of HTSC (YBCO) (approximately 20–30%) and good filler connectivity is crucial, as superconducting particles may stay isolated below the percolation threshold. Interfacial effects and percolation-related transport mechanisms govern conduction in PS composites (*e.g.*, tunnelling, VRH, and ohmic for conductive systems), but the ceramic filler, rather than the polymer itself, promotes superconductivity. There is insufficient of fully integrated systems that combine all functions, but research does point to multifunctional water-treatment potential, such as electrically assisted filtration, adsorption, and photocatalysis.

However, several significant challenges remain in this field. Achieving uniform dispersion of nanofillers, ensuring long-term mechanical and thermal stability, and effectively scaling up synthesis methods are critical for translating laboratory successes into practical applications. Furthermore, research on superconductive polystyrene nanocomposites is still in its early stages, necessitating more comprehensive theoretical modeling

Table 5 Review analysis | proposed and explanation by authors

Topic	Common applications	Enlightenments	References
PS | copolymerization	Effective in cleaning up oil spills by using several polymers in the copolymerization process: polyethylene (PE), polyvinyl chloride (PVC), polyurethane (PU)	Blended PS has been effective in cleaning up oil spills, combines the hydrophobic properties and advantages of their original polymers, leveraging the strengths of each polymer. Showed to be highly more effective than commercially available sorbents towards several types of oil spills. Transforming a hydrophilic substance into an oleophilic adsorbent	39–41
PS | metal NPs	Dye removal as indigo carmine, congo red, rhodamine B, and malachite green, through using iron oxide NPs as a nano filler	*In situ* magnetite precipitation and oxidation produced hybrid mesoporous magnetite (HMM) on polystyrene. Using sulfonated polystyrene and magnetite nanocomposites, dye extracted from solutions efficiently. Co-precipitation produces superparamagnetic spherical magnetite nanoparticles (MNPs). Surface functional groups of sulphonated polystyrene interact with nanoparticles to improve composite synthesis and surface functionalities	53, 54, 57 and 184
	As a catalytic reduction of methylene blue (MB) dye, through using silver NPs as a nano filler	Degradation experiments indicated that hydrophilic alteration introduced sulfonic acid groups, facilitating the fast adsorption of MB by microspheres. In addition, the composite microspheres could enhance the degradation rate of MB by 90–97% because of the presence of silver nanoparticles (Ag NPs), which can catalyze the reduction of MB	59 and 61
PS | chitosan	For mercury (Hg), lead (pb), and cadmium (Cd) removal from aqueous solutions, in the PS copolymerization or nano filler as additives with chitosan	There are functional groups in chitosan's structure that interact strongly with metal ions, such as amine ($-NH_2$) and hydroxyl (–OH). It all comes down to the type of the pollutants; chitosan can remove them whether they are anions or cations. Incorporating nanoparticles doped with chitosan into bio nanocomposites allows for the efficient removal of water pollutants. Because they are protonated, their amino functional groups can bind more strongly to anionic pollutants in acidic conditions. Physical processing of chitosan increases both its surface area and porosity	42, 49 and 62
PS | silica	Organic–inorganic hybrid composites specially which contain silica used in several applications	Organic–inorganic hybrid composites have remarkable catalytic, optical, mechanical, electrical, and magnetic properties. Because of their mechanical properties and morphologies, these composites contain polymer/silica. Silica's porosity, high specific surface area, malleability, and resistivity make it a beneficial material. Hydrophilic silica fillers have several surface groups. Physical and chemical processes can modify precipitated or colloidal silica surfaces. Polymer/silica composites can be used for enzyme immobilisation, dye adsorption, coatings, catalysis, biomedicine, medicine, electronics, and wastewater metal ion removal	35 and 91
PS | PANI	The incorporation of PANI in the PS composites available for removal of ions like arsenic, Hg(II), Cr(VI), and Pb(II)	The amine group in aniline allows it to absorb anions. With so many amine and imine functional groups per unit volume, these polymers should bind to certain metal ions that love nitrogen. Synthesized polyaniline with small dopants (Cl^-, ClO^-, and SO_4^{2-}) showed anion-exchanger behavior due to ion strong affinity metal ions should interact with them. Preserving the mechanical flexibility and initial porosity of purified PS mats is crucial for the most effective techniques of introducing PANI chains to these materials. The nanostructured PANI chains dispersed throughout the PS mat resulted in composites with outstanding electrical properties and well controlled surface-wetting characteristics	131–133

Table 5 (*Contd.*)

Topic	Common applications	Enlightenments	References
PS | CNPs	The PS with CNPs (as: AC, GO, and MWCNT) composite shows promise as an adsorbent for the removal of cationic dyes (as: CV, RhB, and MB) from contaminated water, also toluene, and Pb^{2+} removal	More adsorption sites meant better performance for the activated carbon composite. In addition to being amphiphilic and dispersible, graphene oxide (GO) possesses remarkable mechanical, electrical, and thermal capabilities due to its abundance of hydroxyl, carboxyl, and epoxy groups. Several interlayer negative charges were produced by functional groups that contain oxygen. Electrostatics are able to successfully remove certain cationic contaminants because of this property. Composites loaded with nanofiller (CNP) also showed improvements in modulus, compression strength, foam density, initial weight loss, and maximum decomposition temperature	77 and 134–136

and experimental validation to unlock their potential in energy-efficient electronics and quantum technologies.

The green synthesis of polystyrene nanocomposites employs biological sources, such as plant extracts, microbial processes, or natural waste, to produce nanoparticles for incorporation into polystyrene matrices. This eco-friendly approach offers an alternative to conventional methods, such as microwave-assisted synthesis. Additionally, artificial intelligence (AI) is used to enhance these processes by predicting nanoparticle characteristics, analyzing complex data, and facilitating the design and discovery of innovative polystyrene nanocomposite formulations, thereby accelerating their development for a variety of applications, including troubleshooting and control.

Interdisciplinary collaboration among polymer science, nanotechnology, and condensed matter physics will be essential for creating high-performance, cost-effective, and sustainable conductive and superconductive polymer composites.

Conflicts of interest

There are no conflicts to declare.

List of abbreviations

4NP	4-Nitrophenol
AA	Acrylic acid
AN	Acrylonitrile
AC	Activated carbon
SERS	Active surface-enhanced Raman scattering
AAP	Aminophosphinic acid
APS	Ammonium peroxy disulfate
AI	Artificial intelligence
ATZ	Atrazine
AIBN	Azodiisobutyronitrile
BCS	Bardeen–Cooper–Schrieffer
BCS	Bardeen–Cooper–Schrieffer theory
BPO	Benzoyl peroxide
BC	Biochar
CB	Carbon black
CNPs	Carbon nanoparticles
CNTs	Carbon nanotubes
CMC	Carboxymethyl cellulose
CPC	Cetylpyridinium chloride
CTAB	Cetyltrimethylammonium bromide
CPNs	Clay-polymer nanocomposites
CPs	Conductive polymers
CR	Congo Red dye
CV	Crystal violet dye
DFT	Density functional theory
DMS	Dimethyl sulphate
DVB	Divinylbenzene
EMI	Electromagnetic interference
EPDM	Ethylene propylene diene monomer rubber
EPS	Expanded polystyrene
FIT	Fluctuation-induced tunneling
FCPNC	Fungal chitosan-polystyrene-Co nanocomposites
GPPS	General-purpose polystyrene

GNPs	Graphene nanoplatelets
GO	Graphene oxide
HTSC	High-T_c superconductor
HMM	Hollow mesoporous magnetite
HMSMs	Hollow mesoporous silica microspheres
HPC	Hydroxyl propyl cellulose
HCP	Hyper crosslinked polystyrene
IPNs	Interpenetrating networks
IEX	Ion exchange
LCs	Liquid crystals
ML	Machine learning
NS	Macroporous polystyrene beads
MAC	Magnetic activated carbon
MNPs	Magnetite nanoparticles
MA	Maleic anhydride
MOFs	Metal–organic frameworks
MB	Methylene blue dye
MMT	Montmorillonite
MWCNT	Multi-walled carbon nanotubes
THDACl	*N*,*N*,*N*-Trimethyl-1-hexadecyl ammonium chloride
DFDA	*N*,*N*-Dimethylformamide dimethyl acetal
NZ	Nano zeolites
NPs	Nanoparticles
ODA	Octadecylamine
OV	Octavinyl
OA	Oleic acid
OC	Organoclay
PAH	Poly aromatic hydrocarbon pollutant
PEDOT	Poly(3,4-ethylenedioxythiophene)
PMMA	Poly(methyl methacrylate)
PA	Polyacetylene
PAN	Polyacrylonitrile
PANI	Polyaniline
PAni_ES	Polyaniline emeraldine salt
PDMS	Polydimethylsiloxane
PE	Polyethylene
PFs	Polyfluorenes
POSS	Polyhedral oligomeric silsesquioxane
PP	Polypropylene
PPy	Polypyrrole
PS	Polystyrene
PSIS	Polystyrene derivative
PSFs	Polystyrene fibres
PSW	Polystyrene foam waste
PSMs	Polystyrene microspheres
PSSA	Polystyrene sulfonic acid
SEBS	Polystyrene-*b*-poly(ethylene-*ran*-butylene)-*b*-polystyrene
PSMM	Polystyrene-polymaleic anhydride
PTh	Polythiophene
PU	Polyurethane
PVA	Polyvinyl alcohol
PVC	Polyvinyl chloride
PVDF	Polyvinylidene fluoride
PVP	Polyvinylpyrrolidone
KPS	Potassium persulfate
PW	Produced water
Py	Pyrrole
rGO	Reduced graphene oxide
RAFT	Reversible addition–fragmentation chain transfer polymerization
RhB	Rhodamine B dye
ST	Safranin T
SMP	Shape memory polymer
SMPS	Shape memory polystyrene
AgNP	Silver nanoparticle
SWCNTs	Single-walled carbon nanotubes
SA	Sodium alginate
DBSNa	Sodium dodecyl benzene sulfonate
SDS	Sodium dodecyl sulphate
PSS	Sodium polystyrene sulfonate
ST	Styrene
PSS	Sulfonated polystyrene
SPS	Sulfonated polystyrene
SS	Sulfonated styrene
SWPS	Sulfonated waste polystyrene
SPS	Sulphonated cross-linked polystyrene
YBCO	Superconductor ceramic particles
BSCCO	Superconductor ceramic particles
TEOS	Tetraethyl orthosilicate
TIPS	Thermal-induced phase separation
VRH	Variable-range hopping
XRD	X-ray diffraction
Nano-ZrP	Zirconium phosphate nanoparticles

Data availability

This review compiles and analyzes data from previously published studies on ion-exchange functionalized polystyrene-based composites. No new experimental data were generated. All data are available within the article and its cited references.

References

1 J. Muthukumar, V. A. Kandukuri and R. Chidambaram, A critical review on various treatment, conversion, and disposal approaches of commonly used polystyrene, *Polym. Bull.*, 2024, **81**(4), 2819–2845, DOI: 10.1007/s00289-023-04851-0.

2 A. S. Elgharbawy, Expandable Polystyrene Production and Market Survey- A review, *Egypt. J. Chem.*, 2023, **66**(5), 87–91, DOI: 10.21608/ejchem.2023.137005.6041.

3 P. Jadhav, N. Muhammad and P. Bhuyar, Environmental Technology & Innovation A review on the impact of conductive nanoparticles (CNPs) in anaerobic digestion : Applications and limitations, *Environ. Technol. Innovation*, 2021, **23**, 101526, DOI: 10.1016/j.eti.2021.101526.

4 S. Moulay, Functionalized Polystyrene and Polystyrene-Containing Material Platforms for Various Applications, *Polym.–Plast. Technol. Eng.*, 2017, **0**(0), 1–48, DOI: 10.1080/03602559.2017.1370109.

5 H. Mohammad, A. Ehsani and M. Jalali, Journal of Colloid and Interface Science Electrochemical synthesis of Sm 2 O 3 nanoparticles : Application in conductive polymer

composite films for supercapacitors, *J. Colloid Interface Sci.*, 2017, **505**, 940–946, DOI: 10.1016/j.jcis.2017.06.086.
6 K. W. Pepper, Sulphonated cross-linked polystyrene: A monofunctional cation-exchange resin, *J. Appl. Chem.*, 2007, **1**(3), 124–132, DOI: 10.1002/jctb.5010010307.
7 C. Subramanian, M. Giotto, R. A. Weiss and M. T. Shaw, Chemical cross-linking of highly sulfonated polystyrene electrospun fibers, *Macromolecules*, 2012, **45**(7), 3104–3111, DOI: 10.1021/ma202385g.
8 S. Jiang and B. P. Ladewig, High performance cation exchange membranes synthesized: Via in situ emulsion polymerization without organic solvents and corrosive acids, *J. Mater. Chem. A*, 2019, **7**(29), 17400–17411, DOI: 10.1039/c9ta06248c.
9 L. Chen, Y. Liu, X. Peng, Y. Wei and K. Shao, Simultaneous hypercrosslinking and functionalization of porous polystyrene adsorbent for protein-bound uraemic toxins removal, *React. Funct. Polym.*, 2025, **214**, 106265, DOI: 10.1016/j.reactfunctpolym.2025.106265.
10 A. Singh, A. Chauhan, and R. Gaur, *A Comprehensive Review on the Synthesis , Properties , Environmental Impacts , and Chemiluminescence Applications of Polystyrene (PS)*, Springer Nature, Singapore, 2025, DOI: 10.1007/s44371-025-00125-y.
11 E. Kelpsiene, M. T. Ekvall, M. Lundqvist, O. Torstensson, J. Hua and T. Cedervall, Review of ecotoxicological studies of widely used polystyrene nanoparticles, *Environ. Sci.:Processes Impacts*, 2022, **24**(1), 8–16, DOI: 10.1039/d1em00375e.
12 K. Kik, B. Bukowska and P. Sicińska, Polystyrene nanoparticles: Sources, occurrence in the environment, distribution in tissues, accumulation and toxicity to various organisms, *Environ. Pollut.*, 2020, **262**, DOI: 10.1016/j.envpol.2020.114297.
13 P. Bhaskaran, BCS Theory of Superconductivity: A Conceptual and Application-Oriented Review, *International Journal on Science and Technology*, 2026, **17**(1), 10122, DOI: 10.71097/IJSAT.v17.i1.10122.
14 A. O. Tonoyan and S. P. Davtyan, "High-temperature superconducting ceramic nanocomposites", in *Ceramic Nanocomposites*, Elsevier, 2013, pp. 284–322, DOI: 10.1533/9780857093493.2.284.
15 A. Tonoyan, C. Schick and S. Davtyan, Intercalated Nanocomposites Based on High-Temperature Superconducting Ceramics and Their Properties, *Materials*, 2009, **2**(4), 2154–2187, DOI: 10.3390/ma2042154.
16 V. Kozhevnikov, Meissner Effect: History of Development and Novel Aspects, *J. Supercond. Novel Magn.*, 2021, **34**(8), 1979–2009, DOI: 10.1007/s10948-021-05925-8.
17 Y. V. Fedotov, *et al.*, Magnetic-field and temperature dependence of the critical current in thin epitaxial films of the high-temperature superconductor YBa2Cu3O7−δ, *Low Temp. Phys.*, 2002, **28**(3), 172–183, DOI: 10.1063/1.1468520.
18 R. Abraham, S. Kuryan, J. Isac, A. K. Zacharia, and S. Thomas, "*Yttrium Barium Copper Oxide-Filled Polystyrene as a Dielectric Material*", 2010, DOI: 10.1002/app.
19 Y. A. Vidadi, E. Yanmaz, M. Altunbas and H. Karal, Percolation effects in the diamagnetic response of polystyrene-YBa2Cu3O7−δ superconductor composites, *Phys. C*, 1994, **225**(1–2), 124–126, DOI: 10.1016/0921-4534(94)90335-2.
20 Y. Liu, Y. Zhang, B.-Y. Oh, D.-S. Seo and X. Li, Super-fast switching of liquid crystals sandwiched between highly conductive graphene oxide/dimethyl sulfate doped PEDOT:PSS composite layers, *J. Appl. Phys.*, 2016, **119**(19), 194505, DOI: 10.1063/1.4949488.
21 C. del Río and J. L. Acosta, Extrinsic conducting and superconducting polymer systems. IV. Superconducting properties of YBaCuO composites based on PVDF/PS/carbon black and PVDF/PS/copper polymer systems, *J. Appl. Polym. Sci.*, 1996, **60**(3), 399–405, DOI: 10.1002/(SICI)1097-4628(19960418)60:3<399::AID-APP13>3.0.CO;2-Z.
22 A. N. Ionov, M. P. Volkov, M. N. Nikolaeva, R. Y. Smyslov and A. N. Bugrov, Magnetization of ultraviolet-reduced graphene oxide flakes in composites based on polystyrene, *Materials*, 2021, **14**(10), 1–13, DOI: 10.3390/ma14102519.
23 A. N. Ionov, M. P. Volkov, M. N. Nikolaeva, R. Y. Smyslov and A. N. Bugrov, The magnetization of a composite based on reduced graphene oxide and polystyrene, *Nanomaterials*, 2021, **11**(2), 1–17, DOI: 10.3390/nano11020403.
24 A. Kausar, S. Ahmad and S. M. Salman, Effectiveness of Polystyrene/Carbon Nanotube Composite in Electromagnetic Interference Shielding Materials: A Review, *Polym.-Plast. Technol. Eng.*, 2017, **56**(10), 1027–1042, DOI: 10.1080/03602559.2016.1266367.
25 M. N. Nikolaeva, E. M. Ivan'kova and A. N. Bugrov, Conducting properties of single-wall carbon nanotubes in composites based on poly-styrene, *Nanosyst.:Phys., Chem., Math.*, 2025, **16**(2), 243–249, DOI: 10.17586/2220-8054-2025-16-2-243-249.
26 Y. Zare, M. Naqvi, K. Y. Rhee and S.-J. Park, Unraveling the roles of network and tunnels in the conductivity of carbon nanofiber composites, *Sci. Rep.*, 2025, **15**(1), 35459, DOI: 10.1038/s41598-025-19376-x.
27 E. Barbieri, E. Bilotti, Y. Liu and C. Grimaldi, Pyroresistive response of percolating conductive polymer composites, *Phys. Rev. Mater.*, 2024, **8**(4), 045602, DOI: 10.1103/PhysRevMaterials.8.045602.
28 Y. Zare, M. T. Munir and K. Y. Rhee, Influences of defective interphase and contact region among nanosheets on the electrical conductivity of polymer graphene nanocomposites, *Sci. Rep.*, 2024, **14**(1), 13210, DOI: 10.1038/s41598-024-63981-1.
29 F. Abdollahi, M. Mohammadi, Y. Zare, M. T. Munir, K. Y. Rhee and S. Park, A predictive model for electrical conductivity of polymer carbon black nanocomposites, *Polym. Compos.*, 2025, **46**(8), 7491–7502, DOI: 10.1002/pc.29444.
30 J. Payandehpeyman and M. Mazaheri, Geometrical and physical effects of nanofillers on percolation and electrical conductivity of polymer carbon-based

nanocomposites: a general micro-mechanical model, *Soft Matter*, 2023, **19**(3), 530–539, DOI: 10.1039/D2SM01168A.

31 P. Sheng, E. K. Sichel and J. I. Gittleman, Fluctuation-Induced Tunneling Conduction in Carbon-Polyvinylchloride Composites, *Phys. Rev. Lett.*, 1978, **40**(18), 1197–1200, DOI: 10.1103/PhysRevLett.40.1197.

32 P. Sheng, Fluctuation-induced tunneling conduction in disordered materials, *Phys. Rev. B:Condens. Matter Mater. Phys.*, 1980, **21**(6), 2180–2195, DOI: 10.1103/PhysRevB.21.2180.

33 V. Kažukauskas, V. Kalendra, C. W. Bumby, B. M. Ludbrook and A. B. Kaiser, Electrical conductivity of carbon nanotubes and polystyrene composites, *Phys. Status Solidi C*, 2008, **5**(9), 3172–3174, DOI: 10.1002/pssc.200779193.

34 S. Haider, A. Kausar and B. Muhammad, Overview on Polystyrene/Nanoclay Composite: Physical Properties and Application, *Polym.-Plast. Technol. Eng.*, 2017, **56**(9), 917–931, DOI: 10.1080/03602559.2016.1233563.

35 S. Meer, A. Kausar and T. Iqbal, Attributes of Polymer and Silica Nanoparticle Composites : A Review Attributes of Polymer and Silica Nanoparticle Composites : A Review, *Polym.-Plast. Technol. Eng.*, 2016, **55**(8), 826–861, DOI: 10.1080/03602559.2015.1103267.

36 A. Afzal, A. Kausar and M. Siddiq, Perspectives of Polystyrene Composite with Fullerene, Carbon Black, Graphene, and Carbon Nanotube: A Review, *Polym.-Plast. Technol. Eng.*, 2016, **55**(18), 1988–2011, DOI: 10.1080/03602559.2016.1185632.

37 A. Nasir and A. Kausar, A Review on Materials Derived from Polystyrene and Different Types of Nanoparticles, *Polym.-Plast. Technol. Eng.*, 2015, **54**(17), 1819–1849, DOI: 10.1080/03602559.2015.1038838.

38 S. Kumar and S. Jain, History, introduction, and kinetics of ion exchange materials, *Journal of Chemistry*, 2013, **2013**, 957647, DOI: 10.1155/2013/957647.

39 M. A. Alnaqbi, A. G. Al Blooshi and Y. E. Greish, Polyethylene and Polyvinyl Chloride-Blended Polystyrene Nanofibrous Sorbents and Their Application in the Removal of Various Oil Spills, *Adv. Polym. Technol.*, 2020, **2020**, 1–12, DOI: 10.1155/2020/4097520.

40 N. A. Abdelwahab, N. Shukry and S. F. El-kalyoubi, Separation of emulsified oil from wastewater using polystyrene and surfactant modified sugarcane bagasse wastes blend, *Clean Technol. Environ. Policy*, 2021, **23**(1), 235–249, DOI: 10.1007/s10098-020-01973-1.

41 M. J. Akanbi, S. N. Jayasinghe and A. Wojcik, Characterisation of electrospun PS/PU polymer blend fibre mat for oil sorption, *Polymer*, 2021, **212**, 123129, DOI: 10.1016/j.polymer.2020.123129.

42 T. R. Martins, P. S. Costa, D. A. Bertuol, M. L. Aguiar and E. H. Tanabe, Development of Recycled Expanded Polystyrene Nanofibers Modified by Chitosan for the Removal of Lead(II) from Water, *Metals*, 2022, **12**(8), 1334, DOI: 10.3390/met12081334.

43 D. Li, *et al.*, Aminated polystyrene-polymaleic(anhydride) hollow microsphere membrane for fast and efficient dyes and oils filtration from water, *J. Mater. Chem. A*, 2022, **10**(26), 13936–13945, DOI: 10.1039/d2ta02218d.

44 M. R. El-Aassar, *et al.*, Hybrid Beads of Poly(Acrylonitrile-co-Styrene/Pyrrole)@Poly Vinyl Pyrrolidone for Removing Carcinogenic Methylene Blue Dye Water Pollutant, *J. Polym. Environ.*, 2023, **31**(7), 2912–2929, DOI: 10.1007/s10924-023-02776-3.

45 H. F. Taha, W. A. Gad and I. El-Hussein, Enhanced ammonium removal from aquatic systems by a novel copolymer, *Aqua Water Infrastruct. Ecosyst. Soc.*, 2023, **72**(1), 49–61, DOI: 10.2166/aqua.2022.075.

46 R. Ardelean, A. Popa, A. Visa, E. S. Dragan and C. M. Davidescu, Synthesis, characterization and applications of poly(styrene-co-divinylbenzene) functionalized with aminophosphinic acid pendant groups as high-performance adsorbents for acetylsalicylic acid, *Polym. Bull.*, 2024, **81**(10), 8783–8809, DOI: 10.1007/s00289-023-05123-7.

47 A. Álvarez-Gómez, J. Yuan, J. P. Fernández-Blázquez, V. San-Miguel and M. B. Serrano, Polyacrylonitrile-b-Polystyrene Block Copolymer-Derived Hierarchical Porous Carbon Materials for Supercapacitor, *Polymers*, 2022, **14**(23), 5109, DOI: 10.3390/polym14235109.

48 A. E. Abdelhamid, H. M. Salem, D. A. Ismaeil and A. H. Orabi, Synthesis of ion exchange film based on chemical grafting of styrene onto polyethylene/EPDM rubber blend for thorium removal, *Environ. Monit. Assess.*, 2024, **196**(11), 1–18, DOI: 10.1007/s10661-024-13142-8.

49 B. Porkar, P. A. Atmianlu, M. Mahdavi, M. Baghdadi, H. Farimaniraad and M. A. Abdoli, Chemical modification of polystyrene foam using functionalized chitosan with dithiocarbamate as an adsorbent for mercury removal from aqueous solutions, *Korean J. Chem. Eng.*, 2023, **40**(4), 892–902, DOI: 10.1007/s11814-023-1387-1.

50 M. D. Yadav, *Advanced Nanocomposite Ion Exchange Materials for Water Purification*, Elsevier Inc., 2021, DOI: 10.1016/B978-0-12-821496-1.00014-3.

51 A. Kausar, Shape memory polystyrene-based nanocomposite : present status and future opportunities, *J. Macromol. Sci., Part A:Pure Appl. Chem.*, 2020, **0**(0), 1–10, DOI: 10.1080/10601325.2020.1840919.

52 R. Hosny, A. M. G. Mohamed, O. H. Abdelraheem, M. F. Hussein, M. F. Mubarak and H. A. Ahmed, Synthesis, Characterization, and Adsorption Study of Magnetic Superhydrophobic Monolithic Core-Shell Polystyrene Composite for the Removal of Ethyl Naphthalene from Produced Water Using Fixed Column Bed, *Egypt. J. Chem.*, 2023, **66**(13), 595–608, DOI: 10.21608/EJCHEM.2023.188348.7486.

53 R. W. Abadi, *et al.*, Polystyrene-templated hollow mesoporous magnetite as a bifunctional adsorbent for the removal of rhodamine B via simultaneous adsorption and degradation, *J. Environ. Chem. Eng.*, 2022, **10**(4), 108194, DOI: 10.1016/j.jece.2022.108194.

54 R. Mohammadi, B. Massoumi, R. Mashayekhi and A. Hosseinian, Fe3O4/Polystyrene-Alginate Nanocomposite as a Novel Adsorbent for Highly Efficient Removal of

Dyes, *Iran. J. Chem. Chem. Eng.*, 2022, **41**(11), 3632–3645, DOI: 10.30492/ijcce.2022.529572.4721.

55 N. C. F. Machado, L. A. M. de Jesus, P. S. Pinto, F. G. F. de Paula, M. O. Alves, K. H. A. Mendes, R. V. Mambrini, D. Barrreda, V. Rocha, R. Santamaría, J. P. C. Trigueiro, R. L. Lavall and P. F. R. Ortega, Waste-polystyrene foams-derived magnetic carbon material for adsorption and redox supercapacitor applications, *J. Cleaner Prod.*, 2021, **313**, 127903, DOI: 10.1016/j.jclepro.2021.127903.

56 A. V. Pastukhov, Magnetic sorbents based on hypercrosslinked copolymers of styrene and divinylbenzene with immobilized iron oxides, *React. Funct. Polym.*, 2021, **160**, 104823, DOI: 10.1016/j.reactfunctpolym.2021.104823.

57 C. A. De León-Condés, G. Roa-Morales, G. Martínez-Barrera, P. Balderas-Hernández, C. Menchaca-Campos and F. Ureña-Núñez, A novel sulfonated waste polystyrene/iron oxide nanoparticles composite: Green synthesis, characterization and applications, *J. Environ. Chem. Eng.*, 2019, **7**(1), 102841, DOI: 10.1016/j.jece.2018.102841.

58 A. M. Al-Sabagh, Y. M. Moustafa, A. Hamdy, H. M. Killa, R. T. M. Ghanem and R. E. Morsi, Preparation and characterization of sulfonated polystyrene/magnetite nanocomposites for organic dye adsorption, *Egypt. J. Pet.*, 2018, **27**(3), 403–413, DOI: 10.1016/j.ejpe.2017.07.004.

59 H. Xu, B. Liu and M. Zhang, Synthesis of silver nanoparticles composite mesoporous microspheres for synergistic adsorption-catalytic degradation of methylene blue, *Sep. Purif. Technol.*, 2023, **324**, 124499, DOI: 10.1016/j.seppur.2023.124499.

60 L. Li, S. J. Yu, R. G. Zheng, P. Li, Q. C. Li and J. F. Liu, Removal of iodide anions in water by silver nanoparticles supported on polystyrene anion exchanger, *J. Environ. Sci.*, 2023, **128**, 45–54, DOI: 10.1016/j.jes.2022.08.012.

61 Y. Liu, T. Liu, X. Liu, B. Liu and M. Zhang, Highly loaded silver nanoparticle-modified monodispersed polystyrene composite microspheres (PS/Ag) for rapid catalytic reduction of methylene blue, *Polym. Eng. Sci.*, 2022, **62**(2), 576–585, DOI: 10.1002/pen.25869.

62 S. M. El-Sabbagh, *et al.*, Synthesis of fungal chitosan-polystyrene modified by nanoparticles of binary metals for the removal of heavy metals from waste aqueous media, *RSC Adv.*, 2023, **13**(42), 29735–29748, DOI: 10.1039/d3ra04451c.

63 M. Adel, *et al.*, Decoration of polystyrene with nanoparticles of cobalt hydroxide as new composites for the removal of Fe(iii) and methylene blue from industrial wastewater, *RSC Adv.*, 2023, **13**(36), 25334–25349, DOI: 10.1039/d3ra03794k.

64 V. Srinivasan, V. Sumalatha, A. Prasannan and S. Govindarajan, Utilization of Sulfonated Waste Polystyrene-Based Cobalt Ferrite Magnetic Nanocomposites for Efficient Degradation of Calcon Dye, *Polymers*, 2022, **14**(14), 2909, DOI: 10.3390/polym14142909.

65 N. Khan, *et al.*, Anchoring Zero-Valent Cu and Ni Nanoparticles on Carboxymethyl Cellulose-Polystyrene–Block Polyisoprene–Block Polystyrene Composite Films for Nitrophenol Reduction and Dyes Degradation, *J. Polym. Environ.*, 2023, **31**(2), 608–620, DOI: 10.1007/s10924-022-02579-y.

66 G. Nie, *et al.*, Efficient removal of phosphate by a millimeter-sized nanocomposite of titanium oxides encapsulated in positively charged polymer, *Chem. Eng. J.*, 2019, **360**, 1128–1136, DOI: 10.1016/j.cej.2018.10.184.

67 A. Bakry, M. Adel, A. M. A. El Naggar and M. H. Helal, Nickel hydroxide/polystyrene composites for adsorptive removal of Fe (III) and methylene blue from aqueous solutions, *Egypt. J. Chem.*, 2022, **65**(7), 605–615, DOI: 10.21608/ejchem.2021.105565.4937.

68 M. Pasichnyk, M. Václavíková and I. Melnyk, Fabrication of polystyrene-acrylic/ZnO nanocomposite films for effective removal of methylene blue dye from water, *J. Polym. Res.*, 2021, **28**(2), 1–15, DOI: 10.1007/s10965-021-02418-z.

69 B. M. Thamer, F. A. Al-aizari, H. S. Abdo and M. H. El-Newehy, Upcycling polystyrene foam waste into highly efficient MOF(Cr)-incorporated fiber composite adsorbent to rid water of hazardous dyes, *Chem. Eng. Sci.*, 2025, **311**, 121636, DOI: 10.1016/j.ces.2025.121636.

70 A. Marey, *et al.*, Efficient removal of methylene blue dye from wastewater specimen using polystyrene coated nanoparticles of silica, *Inorg. Chem. Commun.*, 2024, **160**, 112018, DOI: 10.1016/j.inoche.2024.112018.

71 A. Alassod, W. Alkhateeb, I. Alghoraibi, G. Alassod and R. Alassod, Facile fabrication of polystyrene/lignin /OV-POSS nanocomposite monolith by thermally induced phase separation method for wastewater cleanup, *Polym. Bull.*, 2024, **81**, 10081–10118, DOI: 10.1007/s00289-024-05193-1.

72 Z. Dong, *et al.*, Preparation of polystyrene and silane-modified nano-silica superhydrophobic and superoleophilic three-dimensional composite fiber membranes for efficient oil absorption and oil-water separation, *J. Environ. Chem. Eng.*, 2024, **12**(3), 112690, DOI: 10.1016/j.jece.2024.112690.

73 S. Jamalpour, A. Azizi, A. Chehrazi and R. Maghsoudi, Superhydrophobic/superoleophilic polyurethane sponge modified by synthesized SiO2-poly(styrene-co-oleic acid) organic-inorganic nanoparticle for efficient oil-water separation, *Colloids Surf., A*, 2024, **703**, 135269, DOI: 10.1016/j.colsurfa.2024.135269.

74 R. Abouzeid, H. Dardeer, M. Mahgoub and A. Abdelkader, Adsorption of cationic methylene blue dye on polystyrene sulfonic acid composites from waste: Kinetics and equilibrium, *Egypt. J. Chem.*, 2021, 210925, DOI: 10.21608/ejchem.2021.104402.4822.

75 J. Wang, *et al.*, Determination of organochlorine pesticide residues in food by polystyrene coated silica magnetic microspheres combined with gas chromatography-mass spectrometry, *Microchem. J.*, 2024, **207**, 112077, DOI: 10.1016/j.microc.2024.112077.

76 F. Damavandi and J. B. P. Soares, Polystyrene magnetic nanocomposite blend: An effective, facile, and economical alternative in oil spill removal applications, *Chemosphere*,

2022, **286**, 131611, DOI: 10.1016/j.chemosphere.2021.131611.

77 T. A. Abdullah, *et al.*, Polystyrene-Fe3O4-MWCNTs Nanocomposites for Toluene Removal from Water, *Materials*, 2021, **14**(19), 5503, DOI: 10.3390/ma14195503.

78 M. Yoonessi, B. A. Lerch, J. A. Peck, R. B. Rogers, F. J. Sola, and M. A. Meador, "*Self-Healing of Core–Shell Magnetic Polystyrene Nanocomposites*", 2015, DOI: 10.1021/acsami.5b04314.

79 Z. T. Mengesha and J. Yang, Silver Nanoparticle-Decorated Shape-Memory Polystyrene Sheets as Highly Sensitive Surface-Enhanced Raman Scattering Substrates with a Thermally Inducible Hot Spot Effect, *Anal. Chem.*, 2016, **88**(22), 10908–10915, DOI: 10.1021/acs.analchem.6b02256.

80 D. Amoabeng and S. S. Velankar, Bulk soldering: Conductive polymer composites filled with copper particles and solder, *Colloids Surf., A*, 2018, **553**, 624–632, DOI: 10.1016/j.colsurfa.2018.06.013.

81 K. Tian, C. Liu, H. Yang and X. Ren, Colloids and Surfaces A : Physicochemical and Engineering Aspects In situ synthesis of copper nanoparticles/polystyrene composite, *Colloids Surf., A*, 2012, **397**, 12–15, DOI: 10.1016/j.colsurfa.2012.01.019.

82 W. Wang, Y. Liu, and J. Leng, "*Influence of the Ultraviolet Irradiation on the Properties of TiO 2 -polystyrene Shape Memory Nanocomposites*", ed. J. A. Epaarachchi, A. K. Lau, and J. Leng, 2013, p. 879315, DOI: 10.1117/12.2027860.

83 Q. Zhang, B. Pan, S. Zhang, J. Wang, W. Zhang and L. Lv, New insights into nanocomposite adsorbents for water treatment: A case study of polystyrene-supported zirconium phosphate nanoparticles for lead removal, *J. Nanopart. Res.*, 2011, **13**(10), 5355–5364, DOI: 10.1007/s11051-011-0521-x.

84 A. A. Ayalew, A critical review on clay-based nanocomposite particles for application of wastewater treatment, *Water Sci. Technol.*, 2022, **85**(10), 3002–3022, DOI: 10.2166/wst.2022.150.

85 A. Amari, F. M. Alzahrani, K. M. Katubi, N. S. Alsaiari, M. A. Tahoon and F. Ben Rebah, Clay-polymer nanocomposites: Preparations and utilization for pollutants removal, *Materials*, 2021, **14**(6), 1–21, DOI: 10.3390/ma14061365.

86 B. Xu *et al.*, "*Thermo-mechanical Properties of Polystyrene-Based Shape Memory Nanocomposites †*", 2010, pp. 3442–3448, DOI: 10.1039/b923238a.

87 J. Aseeri, N. M. Alandis, W. Mekhamer and M. Alam, Miscibility studies of polystyrene/polyvinyl chloride blend in presence of organoclay, *Open Chem.*, 2019, **17**(1), 927–935, DOI: 10.1515/chem-2019-0095.

88 F. D. Alsewailem and S. A. Aljlil, Recycled Polymer/Clay Composites for Heavy-Metals Adsorption, *Mater. Tehnol.*, 2013, **47**(4), 525–529.

89 A. M. Khalil and S. H. Kenawy, Hybrid membranes based on clay-polymer for removing methylene blue from water, *Acta Chim. Slov.*, 2020, **67**(1), 96–104, DOI: 10.17344/acsi.2019.5227.

90 A. A. El Mansoub, H. A. Hani, M. M. El Sayed, A. M. G. Abulnour, H. M. Fahmy and R. M. El Nashar, Microwave-Assisted Synthesis of Sulfonated Polystyrene Composite Resins for the Removal of Cationic Dyes, *Egypt. J. Chem.*, 2025, **51**, 621–641, DOI: 10.21608/ejchem.2025.384154.11778.

91 D. Nartop and Ç. Kazak, Synthesis and characterization of novel polystyrene-silica composites containing azomethine, *J. Mol. Struct.*, 2021, **1227**, 129705, DOI: 10.1016/j.molstruc.2020.129705.

92 X. Li, X. Wan and Q. Ma, Preparation of Hollow Mesoporous Silica Microspheres Using Polystyrene Microspheres as Templates, *Arabian J. Sci. Eng.*, 2025, 14823–14833, DOI: 10.1007/s13369-024-09918-2.

93 H. A. Shirinova, A. E. Surkhayli, B. G. Pashayev, H. M. Mammadov, M. A. Jafarov and L. R. Gahramanli, Preparation, characterization and thermal properties of the PS+Si based polymer nanocomposites, *J. Thermoplast. Compos. Mater.*, 2025, **38**(5), 1785–1798, DOI: 10.1177/08927057241288195.

94 X. Fan, L. Niu and Z. Xia, Preparation of raspberry-like silica microcapsules via sulfonated polystyrene template and aniline medium assembly method, *Colloid Polym. Sci.*, 2014, **292**(12), 3251–3259, DOI: 10.1007/s00396-014-3377-7.

95 H. T. Ip, L. Liu, L. Hong and T. Ngai, Synthesis of polystyrene/silica and poly(styrene-co-butyl acrylate)/silica nanocomposite particles by Pickering emulsion polymerization with non-functionalized silica nanoparticles, *Colloids Surf., A*, 2022, **654**, 130104, DOI: 10.1016/j.colsurfa.2022.130104.

96 M. Mocan and N. Uyanık, Polystyrene-Organoclay Nanocomposites Prepared via In-Situ Emulsion Polymerization, *Polym. Polym. Compos.*, 2013, **21**(3), 151–156, DOI: 10.1177/096739111302100305.

97 M. Mirzataheri, S. Khamisabadi and A. Salimi, Characterization of styrene- co -butyl acrylate/Cloisite Na + nanocomposite film synthesized via soap free emulsion polymerization, *Prog. Org. Coat.*, 2016, **99**, 274–281, DOI: 10.1016/j.porgcoat.2016.06.006.

98 M. Ghasemzadeh, A. Nodehi and H. Ebadi-Dehaghani, The Effect of Structure of the Clay Modifier on the Morphology and Properties of Polystyrene/Clay Nanocomposites Prepared via In Situ Suspension Polymerization, *J. Macromol. Sci., Part B:Phys.*, 2014, **53**(8), 1364–1376, DOI: 10.1080/00222348.2014.931192.

99 P. P. Nair and S. Beevi B, Investigation of compatibility of nanofillers and catalysts for the synthesis of polystyrene nanocomposites, *International Journal of Emerging Technologies and Innovative Research*, 2017, **4**, 1017–1024.

100 U. Yilmazer and G. Ozden, Polystyrene–organoclay nanocomposites prepared by melt intercalation, in situ, and masterbatch methods, *Polym. Compos.*, 2006, **27**(3), 249–255, DOI: 10.1002/pc.20191.

101 A. Kausar, "Essence of nanoparticles and functional nanofillers for conducting polymers", in *Conducting Polymer-Based Nanocomposites*, Elsevier, 2021, pp. 57–76, DOI: 10.1016/B978-0-12-822463-2.00001-4.

102 M. A. Ashraf, W. Peng, Y. Zare and K. Y. Rhee, Effects of Size and Aggregation/Agglomeration of Nanoparticles on the Interfacial/Interphase Properties and Tensile Strength of Polymer Nanocomposites, *Nanoscale Res. Lett.*, 2018, **13**(1), 214, DOI: 10.1186/s11671-018-2624-0.

103 C. M. Liauw, G. C. Lees, R. N. Rothon, A. N. Wilkinson and P. Limpanapittayatorn, Evaluation of an alternative modification route for layered silicates and synthesis of poly(styrene) layered silicate nanocomposites by in-situ suspension polymerisation, *Compos. Interfaces*, 2007, **14**(4), 361–386, DOI: 10.1163/156855407780452896.

104 D. J. Carastan, A. Vermogen, K. Masenelli-Varlot and N. R. Demarquette, Quantification of clay dispersion in nanocomposites of styrenic polymers, *Polym. Eng. Sci.*, 2010, **50**(2), 257–267, DOI: 10.1002/pen.21527.

105 M. M. Rahman, K. H. Khan, M. M. H. Parvez, N. Irizarry and M. N. Uddin, Polymer Nanocomposites with Optimized Nanoparticle Dispersion and Enhanced Functionalities for Industrial Applications, *Processes*, 2025, **13**(4), 994, DOI: 10.3390/pr13040994.

106 A. Moreno and M. H. Sipponen, Overcoming Challenges of Lignin Nanoparticles: Expanding Opportunities for Scalable and Multifunctional Nanomaterials, *Acc. Chem. Res.*, 2024, **57**(14), 1918–1930, DOI: 10.1021/acs.accounts.4c00206.

107 S. Jha, B. Akula, H. Enyioma, M. Novak, V. Amin and H. Liang, Biodegradable Biobased Polymers: A Review of the State of the Art, Challenges, and Future Directions, *Polymers*, 2024, **16**(16), 2262, DOI: 10.3390/polym16162262.

108 R. Kumar, *et al.*, An investigation of the environmental implications of bioplastics: Recent advancements on the development of environmentally friendly bioplastics solutions, *Environ. Res.*, 2024, **244**, 117707, DOI: 10.1016/j.envres.2023.117707.

109 M. T. Hossain, *et al.*, Research and application of polypropylene: a review, *Discover Nano*, 2024, **19**(1), 2, DOI: 10.1186/s11671-023-03952-z.

110 O. A. Moskalyuk, A. V. Belashov, A. A. Zhikhoreva, Y. M. Beltukov and I. V. Semenova, Mechanical Performance of Polystyrene-Based Nanocomposites Filled with Carbon Allotropes, *Appl. Sci.*, 2023, **13**(6), 4022, DOI: 10.3390/app13064022.

111 K. Gündoğan and D. Karaağaç, Multi-Walled Carbon Nanotube (MWCNT)-Reinforced Polystyrene (PS) Composites: Preparation, Structural Analysis, and Mechanical and Thermal Properties, *Polymers*, 2025, **17**(14), 1917, DOI: 10.3390/polym17141917.

112 M. Ismail, M. Bayoumi and S. Akl, Influence of incorporation carbon nanoparticles CNP on the mechanical properties of polystyrene composite, *Res. Eng. Struct. Mater.*, 2024, 789–799, DOI: 10.17515/resm2023.37me0823rs.

113 J. Zhang, H. Liu, S. S. Sablani and Q. Wu, Recycling Functional Fillers from Waste Tires for Tailored Polystyrene Composites: Mechanical, Fire Retarding, Electromagnetic Field Shielding, and Acoustic Insulation Properties—A Short Review, *Materials*, 2024, **17**(11), 2675, DOI: 10.3390/ma17112675.

114 Z. Li, M. Liu and R. J. Young, Dependence of the reinforcement of polymer-based nanocomposites upon the nanofiller geometry, *Nano Mater. Sci.*, 2024, DOI: 10.1016/j.nanoms.2024.04.014.

115 Z. G. Mohammadsalih, N. Mullin, S. Amarie, A. Danilov and I. Ur Rehman, Nanomechanical behavior of polystyrene/graphene oxide nanocomposites, *Fullerenes, Nanotubes Carbon Nanostruct.*, 2024, **32**(1), 106–118, DOI: 10.1080/1536383X.2023.2263597.

116 Z. G. Mohammadsalih, V. Uddin Siddiqui and S. M. Sapuan, The role of organic solvent and nano-additives loading in preparing and characterizing graphene oxide based polystyrene nanocomposites, *Polym.-Plast. Technol. Mater.*, 2024, **63**(9), 1175–1186, DOI: 10.1080/25740881.2024.2325431.

117 M. Fatima, *et al.*, Evaluation of a novel composite of expanded polystyrene with rGO and SEBS-g-MA, *Microsc. Res. Tech.*, 2024, **87**(8), 1965–1973, DOI: 10.1002/jemt.24567.

118 S. P. Thomas, Interaction of silica with polystyrene: mechanical properties, polymer/filler adhesion and failure behavior, *Chim. Techno Acta*, 2024, **11**(1), 11105, DOI: 10.15826/chimtech.2024.11.1.05.

119 S. Amira, Z. Belkacem, S. Terchi and G. Benaiche, Enhancement of Polystyrene Nanocomposites with THDACl-Modified Montmorillonite via Melt Compounding, *Ann. Chim.-Sci. Mat.*, 2024, **48**(2), 251–258, DOI: 10.18280/acsm.480211.

120 Z. Khiati, L. Mrah and A. Mezrai, Improvement of the thermal and mechanical behaviour of polystyrene (PS)-based nanocomposite films by modification of the composition and type of nanofiller, *Int. Polym. Process.*, 2024, **39**(5), 580–590, DOI: 10.1515/ipp-2024-0089.

121 S. Ur Rehman, S. Javaid, M. Shahid, T. Yasin and B. Rashid, Flame Retardant Nanocomposites of Polystyrene-Modified Sepiolite Clay, *MATEC Web Conf.*, 2023, **381**, 02002, DOI: 10.1051/matecconf/202338102002.

122 A. Akelah, A. Rehab, H. Harhash, M. A. Abdelwahab and H. S. A. Mandour, Nanocomposites of organo-montmorillonite/polystyrene latex particles via free radical miniemulsion polymerization, *RSC Adv.*, 2025, **15**(7), 5537–5546, DOI: 10.1039/D4RA08943J.

123 A. F. Osman, M. S. Badawi, M. Roumie and R. Awad, Effect of PbO Incorporation with Different Particle Sizes on Structural and Mechanical Properties of Polystyrene, *Mater. Perform. Charact.*, 2023, **12**(1), 23–44, DOI: 10.1520/MPC20220070.

124 A. Fadhil Kadhim and A. Hashim, Recent review on metal oxides nanostructures doped polystyrene for biological and industrial applications, *World J. Adv. Res. Rev.*, 2023, **17**(3), 412–423, DOI: 10.30574/wjarr.2023.17.3.0404.

125 S. Baranek, V. Cerny, R. Drochytka, L. Meszarosova and J. Melichar, Electrically conductive composite materials with incorporated waste and secondary raw materials, *Sci. Rep.*, 2023, **13**(1), 1–23, DOI: 10.1038/s41598-023-36287-x.

126 M. A. Shahid, *et al.*, Advances in Conductive Polymer-Based Flexible Electronics for Multifunctional Applications, *J. Compos. Sci.*, 2025, **9**(1), 1–34, DOI: 10.3390/jcs9010042.
127 X. Y. Qi, *et al.*, Enhanced electrical conductivity in polystyrene nanocomposites at ultra-low graphene content, *ACS Appl. Mater. Interfaces*, 2011, **3**(8), 3130–3133, DOI: 10.1021/am200628c.
128 A. Tarhini and A. R. Tehrani-Bagha, Advances in Preparation Methods and Conductivity Properties of Graphene-based Polymer Composites, *Appl. Compos. Mater.*, 2023, **30**(6), 1737–1762, DOI: 10.1007/s10443-023-10145-5.
129 V. Babel and B. L. Hiran, A review on polyaniline composites: Synthesis, characterization, and applications, *Polym. Compos.*, 2021, **42**(7), 3142–3157, DOI: 10.1002/pc.26048.
130 P. Azmoon, M. Farhadian, A. Pendashteh and A. H. Navarchian, Fabrication of porous and conductive polystyrene/polyaniline fibers via electrospinning method: Adsorption and selectivity of oil, *J. Polym. Res.*, 2025, **32**(3), 1–13, DOI: 10.1007/s10965-025-04299-y.
131 J. J. Alcaraz-Espinoza, A. E. Chávez-Guajardo, J. C. Medina-Llamas, C. A. S. Andrade and C. P. de Melo, Hierarchical Composite Polyaniline–(Electrospun Polystyrene) Fibers Applied to Heavy Metal Remediation, *ACS Appl. Mater. Interfaces*, 2015, **7**(13), 7231–7240, DOI: 10.1021/acsami.5b00326.
132 B. Davodi and M. Jahangiri, Determination of optimum conditions for removal of As (III) and As (V) by polyaniline/polystyrene nanocomposite, *Synth. Met.*, 2014, **194**, 97–101, DOI: 10.1016/j.synthmet.2014.04.020.
133 M. S. Lashkenari, B. Davodi, M. Ghorbani and H. Eisazadeh, Use of core-shell polyaniline/polystyrene nanocomposite for removal of Cr (VI), *High Perform. Polym.*, 2012, **24**(5), 345–355, DOI: 10.1177/0954008311436222.
134 B. M. Thamer, F. A. Al-aizari, H. S. Abdo and A. M. Al-Enizi, Activated carbon-decorated electrospun polystyrene fibers for highly efficient removal of hazardous crystal violet dye from water, *Colloids Surf., A*, 2024, **688**, 133612, DOI: 10.1016/j.colsurfa.2024.133612.
135 A. Kausar, Structure and Properties of Polyacrylonitrile/Polystyrene and Carbon Nanoparticle-Based Nanocomposite Foams, *Adv. Mater. Sci.*, 2019, **19**(1), 5–20, DOI: 10.2478/adms-2019-0001.
136 W. Chen, J. Luan, X. Yu, X. Wang and X. Ke, Preparation of core-shell structured polystyrene @ graphene oxide composite microspheres with high adsorption capacity and its removal of dye contaminants, *Environ. Technol.*, 2021, **42**(24), 3840–3851, DOI: 10.1080/09593330.2020.1743372.
137 A. Samadi, M. Xie, J. Li, H. Shon, C. Zheng and S. Zhao, Polyaniline-based adsorbents for aqueous pollutants removal: A review, *Chem. Eng. J.*, 2021, **418**, 129425, DOI: 10.1016/j.cej.2021.129425.
138 N. Sharma, A. Singh, N. Kumar, A. Tiwari, M. Lal and S. Arya, A review on polyaniline and its composites: from synthesis to properties and progressive applications, *J. Mater. Sci.*, 2024, **59**(15), 6206–6244, DOI: 10.1007/s10853-024-09562-z.
139 S. Senguttuvan, P. Senthilkumar, V. Janaki and S. Kamala-Kannan, Significance of conducting polyaniline based composites for the removal of dyes and heavy metals from aqueous solution and wastewaters - A review, *Chemosphere*, 2021, **267**, 129201, DOI: 10.1016/j.chemosphere.2020.129201.
140 E. Eskandari, M. Kosari, M. H. D. A. Farahani and N. D. Khiavi, A review on polyaniline-based materials applications in heavy metals removal and catalytic processes, *Sep. Purif. Technol.*, 2020, **231**, 115901, DOI: 10.1016/j.seppur.2019.115901.
141 P. Duan, D. Mao, D. Zhang, X. Wang, X. Kong and Y. Piao, Polyaniline and polystyrene sulfonic acid modified on conductive biochar nanoparticle with strong signal enhancement for trace atrazine detection, *Electrochim. Acta*, 2023, **468**, 143198, DOI: 10.1016/j.electacta.2023.143198.
142 P. Stelmaszczyk, M. Iwan, D. Pawcenis and R. Wietecha-Posłuszny, Comparison of ZrO2 Particles and Polyaniline as Additives in Polystyrene-Based Sorbents for the Micro-Solid Phase Extraction of Psychoactive Drugs from Biofluids, *Molecules*, 2024, **29**(4), 761, DOI: 10.3390/molecules29040761.
143 S. Uzunçar, L. Meng, A. P. F. Turner and W. C. Mak, Processable and nanofibrous polyaniline:polystyrene-sulphonate (nano-PANI:PSS) for the fabrication of catalyst-free ammonium sensors and enzyme-coupled urea biosensors, *Biosens. Bioelectron.*, 2021, **171**, 112725, DOI: 10.1016/j.bios.2020.112725.
144 V. A. Kabanova, O. L. Gribkova, S. I. Pozin, V. A. Tverskoy and A. A. Nekrasov, Complexes of Polyaniline with Sulfonated Polysulfone. Their Structure and Sensory Properties, *Prot. Met. Phys. Chem. Surf.*, 2024, **60**(2), 148–157, DOI: 10.1134/S2070205124701715.
145 Q. Zhang, *et al.*, In-situ coating PVDF membrane by polystyrene sulfonic acid doped polyaniline to improve its anti-fouling performance and acid resistance, *Appl. Surf. Sci.*, 2024, **652**, 159339, DOI: 10.1016/j.apsusc.2024.159339.
146 T. Jiao, *et al.*, From white pollution to green coating—PS/PANI anti-corrosive coatings from waste PS foams, *Chem. Eng. J.*, 2024, **487**, 150383, DOI: 10.1016/j.cej.2024.150383.
147 A. M. Mocioiu, I. A. Tudor and O. C. Mocioiu, Application of polyaniline for flexible semiconductors, *Coatings*, 2021, **11**(1), 1–10, DOI: 10.3390/coatings11010049.
148 F. Z. Hamlaoui and N. Naar, Characterization of polyaniline/polystyrene blends prepared by three different methods, *Chem. Pap.*, 2021, **75**(4), 1431–1443, DOI: 10.1007/s11696-020-01395-9.
149 M. Das, T. K. Pani and B. Sundaray, Electrical properties of solution cast films of polystyrene/polyaniline-multiwalled carbon nanotube nanocomposites, *Compos., Part C: Open Access*, 2020, **2**, 100025, DOI: 10.1016/j.jcomc.2020.100025.
150 L. Zhang, T. Hao, S. Song, B. Wang, D. Liu, Z. Ren, W. Liu, Y. Zhang, G. Xu, X. Yan, Y. Lu and Y. Li, Enhancing infrared

electrochromic properties of the poly(styrene sulfonate) doped polyaniline composite film by morphology regulation, *Chem. Eng. J.*, 2023, **475**, 145927, DOI: 10.1016/j.cej.2023.145927.

151 J. Bhadra and N. Al-Thani, Advances in blends preparation based on electrically conducting polymer, *Emergent Mater.*, 2019, **2**(1), 67–77, DOI: 10.1007/s42247-019-00027-7.

152 L. Ahmadkhani, *et al.*, Development and characterization of a novel conductive polyaniline-g-polystyrene/Fe3O4 nanocomposite for the treatment of cancer, *Artif. Cells, Nanomed., Biotechnol.*, 2019, **47**(1), 873–881, DOI: 10.1080/21691401.2019.1575839.

153 J. P L, H. Nallabothula, A. V Menon and S. Bose, Nanoinfiltration for Enhancing Microwave Attenuation in Polystyrene–Nanoparticle Composites, *ACS Appl. Nano Mater.*, 2020, **3**(2), 1872–1880, DOI: 10.1021/acsanm.9b02521.

154 W. Yang, W. Zou, Z. Du, H. Li and C. Zhang, Enhanced conductive polymer nanocomposite by foam structure and polyelectrolyte encapsulated on carbon nanotubes, *Compos. Sci. Technol.*, 2016, **123**, 106–114, DOI: 10.1016/j.compscitech.2015.12.009.

155 N. Ahmed, A. Kausar and B. Muhammad, Shape memory properties of electrically conductive multi-walled carbon nanotube-filled polyurethane/modified polystyrene blends, *J. Plast. Film Sheeting*, 2016, **32**(3), 272–292, DOI: 10.1177/8756087915595454.

156 B. H. Rabee and A. Hashim, Synthesis and Characterization of Carbon Nanotubes -Polystyrene Composites, *European Journal of Scientific Research*, 2011, **60**(2), 247–254.

157 A. Kausar, "*Technical Viewpoint on Polystyrene/Graphene Nanocomposite*", 2022, DOI: 10.1177/0892705720907653.

158 R. Farouq, Functionalized graphene/polystyrene composite , green synthesis and characterization, *Sci. Rep.*, 2022, 1–7, DOI: 10.1038/s41598-022-26270-3.

159 Y.-H. Yu, Y.-Y. Lin, C.-H. Lin, C.-C. Chan and Y.-C. Huang, High-performance polystyrene/graphene-based nanocomposites with excellent anti-corrosion properties, *Polym. Chem.*, 2014, **5**(2), 535–550, DOI: 10.1039/C3PY00825H.

160 W. Li, X. Tang, H. Zhang, Z. Jiang and Z. Yu, Simultaneous surface functionalization and reduction of graphene oxide with octadecylamine for electrically conductive polystyrene composites, *Carbon*, 2011, **49**(14), 4724–4730, DOI: 10.1016/j.carbon.2011.06.077.

161 M. Fathy, T. Abdel Moghny, A. E. Awad Allah and A. E. Alblehy, Cation exchange resin nanocomposites based on multi-walled carbon nanotubes, *Appl. Nanosci.*, 2014, **4**(1), 103–112, DOI: 10.1007/s13204-012-0178-5.

162 J. L. Apátiga, *et al.*, Non-Covalent Interactions on Polymer-Graphene Nanocomposites and Their Effects on the Electrical Conductivity, *Polymers*, 2021, **13**(11), 1714, DOI: 10.3390/polym13111714.

163 Y. Han, *et al.*, Molecular dynamics simulation of the formation mechanism of the thermal conductive filler network of polymer nanocomposites, *Phys. Chem. Chem. Phys.*, 2022, **24**(7), 4334–4347, DOI: 10.1039/D1CP03276C.

164 D. Petras, P. Slobodian, R. Olejnik and P. Riha, Temperature Dependence of Electrical Conductivity of Multi-Walled Carbon Nanotube Networks in a Polystyrene Composite, *Key Eng. Mater.*, 2013, **543**, 356–359, DOI: 10.4028/www.scientific.net/KEM.543.356.

165 J. Francis, N. P. Vaisakh, and C. S. S. Sangeeth, "*Temperature Dependent Charge Transport in Polymer-Carbon Nanotube and Polymer-Reduced Graphene Oxide Composites: A Comparison*", 2019, p, 020016, DOI: 10.1063/1.5130226.

166 G. Ambrosetti, I. Balberg and C. Grimaldi, Percolation-to-hopping crossover in conductor-insulator composites, *Phys. Rev. B:Condens. Matter Mater. Phys.*, 2010, **82**(13), 134201, DOI: 10.1103/PhysRevB.82.134201.

167 Ö. B. Mergen, E. Umut, E. Arda and S. Kara, A comparative study on the AC/DC conductivity, dielectric and optical properties of polystyrene/graphene nanoplatelets (PS/GNP) and multi-walled carbon nanotube (PS/MWCNT) nanocomposites, *Polym. Test.*, 2020, **90**, 106682, DOI: 10.1016/j.polymertesting.2020.106682.

168 T. Huxley, "Electrical engineering perspective on superconductors", in *Fundamentals of Electromagnetic Levitation: Engineering Sustainability through Efficiency*, Institution of Engineering and Technology, 2012, pp. 113–133, DOI: 10.1049/PBCS024E_ch6.

169 B. A. Glowacki, "Superconductivity and Superconductors", in *Kirk-Othmer Encyclopedia of Chemical Technology*, Wiley, 2005, DOI: 10.1002/0471238961.supeglow.a01.

170 J. Fleiter, I. Falorio, and A. Ballarino, "*Superconductivity 1 JUAS 2020-Practical Work Day at CERN*", 2020, pp. 1–16.

171 Y. Xiang, Q. Li, Y. Li, H. Yang, Y. Nie and H. H. Wen, Physical Properties Revealed by Transport Measurements for Superconducting Nd0.8Sr0.2NiO2Thin Films, *Chin. Phys. Lett.*, 2021, **38**(4), 0–8, DOI: 10.1088/0256-307X/38/4/047401.

172 D. Kaplan, A. Zheng, J. Blawat, R. Jin, R. J. Cava, V. Oudovenko, G. Kotliar, A. M. Sengupta and W. Xie, Deep learning-based superconductivity prediction and experimental tests, *Eur. Phys. J. Plus*, 2025, **140**(1), 58, DOI: 10.1140/epjp/s13360-024-05947-w.

173 S. G. Jung, G. Jung and J. M. Cole, Machine-Learning Predictions of Critical Temperatures from Chemical Compositions of Superconductors, *J. Chem. Inf. Model.*, 2024, **64**(19), 7349–7375, DOI: 10.1021/acs.jcim.4c01137.

174 J. A. Alarco, P. C. Talbot and I. D. R. Mackinnon, Identification of superconductivity mechanisms and prediction of new materials using Density Functional Theory (DFT) calculations, *J. Phys.:Conf. Ser.*, 2018, **1143**(1), 012028, DOI: 10.1088/1742-6596/1143/1/012028.

175 J. Zhang, *et al.*, An integrated machine learning model for accurate and robust prediction of superconducting critical temperature, *J. Energy Chem.*, 2023, **78**, 232–239, DOI: 10.1016/j.jechem.2022.11.047.

176 P. A. H. Nawoda, G. P. Hettiarachchi and M. D. T. Attygalle, Predicting the critical temperature of superconductors and materials classification with a balanced dataset without

prior knowledge, *J. Appl. Phys.*, 2026, **139**(2), 023903, DOI: 10.1063/5.0290299.

177 S. Lee, J. Hattrick-Simpers, Y.-J. Kim and O. Anatole von Lilienfeld, High- Tc superconductor candidates proposed by machine learning, *Mach. Learn. Sci. Technol.*, 2025, **6**(3), 035052, DOI: 10.1088/2632-2153/ae04c1.

178 K. Rientong, N. Natkunlaphat and U. Pinsook, Analysis of superconducting critical temperature using numerical method, *J. Phys.:Conf. Ser.*, 2023, **2653**(1), 012054, DOI: 10.1088/1742-6596/2653/1/012054.

179 Z. Mahdi, A. El Hanandeh and Q. J. Yu, Electro-assisted adsorption of heavy metals from aqueous solutions by biochar, *Water Sci. Technol.*, 2020, **81**(4), 801–812, DOI: 10.2166/wst.2020.163.

180 Y. Xiong, *et al.*, Interfacial interaction between micro/nanoplastics and typical PPCPs and nanoplastics removal via electrosorption from an aqueous solution, *Water Res.*, 2020, **184**, 116100, DOI: 10.1016/j.watres.2020.116100.

181 J. Ding, P. Zhang, S. Fang, F. Zhang, Q. Xia, Y. Bu, P. Shen, X. Zhang, C. Wang, C. D Vecitis and G. Gao, Conductive Adsorbent for Electrically Controlled Desorption and Sequential Release of Aqueous Mixture, *Adv. Funct. Mater.*, 2024, **34**(48), 2408274, DOI: 10.1002/adfm.202408274.

182 S. Wanjale, *et al.*, Surface tailored PS/TiO2 composite nanofiber membrane for copper removal from water, *J. Colloid Interface Sci.*, 2016, **469**, 31–37, DOI: 10.1016/j.jcis.2016.01.054.

183 Y. Ren, Z. Lin, X. Mao, W. Tian, T. Van Voorhis and T. A. Hatton, Superhydrophobic, Surfactant-doped, Conducting Polymers for Electrochemically Reversible Adsorption of Organic Contaminants, *Adv. Funct. Mater.*, 2018, **28**(32), 1801466, DOI: 10.1002/adfm.201801466.

184 A. M. Al-sabagh, Y. M. Moustafa, A. Hamdy, H. M. Killa, R. T. M. Ghanem and R. E. Morsi, Preparation and characterization of sulfonated polystyrene/magnetite nanocomposites for organic dye adsorption, *Egypt. J. Pet.*, 2018, **27**(3), 403–413, DOI: 10.1016/j.ejpe.2017.07.004.